Spectroscopy, electrochemistry and antiproliferative properties of Au(III), Pt(II) and Cu(II) complexes bearing modified 2,2′:6′,2′′-terpyridine ligands. Impact of metal center and substituent incorporated into terpy framework

Anna Maroń[a], Katarzyna Czerwińska[a], Barbara Machura[a,*], Luis Raposo[b], Catarina Roma-Rodrigues[b], Alexandra R Fernandes[b,*], Jan Grzegorz Małecki[a], Agata Szlapa-Kula[c], Slawomir Kula[d], Stanisław Krompiec[c]

[a.] *Department of Crystallography, Institute of Chemistry, University of Silesia, 9th Szkolna St., 40-006 Katowice, Poland. Email: barbara.machura@us.edu.pl*
[b.] *UCIBIO, Departamento de Ciências da Vida, Faculdade de Ciências e Tecnologia, Universidade NOVA de Lisboa, Campus de Caparica, 2829-516 Caparica, Portugal. Email: ma.fernandes@fct.unl.pt*
[c.] *Department of Inorganic, Organometallic Chemistry and Catalysis, Institute of Chemistry, University of Silesia, 9th Szkolna St., 40-006 Katowice, Poland.*
[d.] *Department of Polymer Chemistry, Institute of Chemistry, University of Silesia, 9th Szkolna St., 40-006 Katowice, Poland*

Supplementary information

Table of Contents

Table S1. Short intra- and intermolecular hydrogen bonds detected in complexes.

D–H•••A	D–H [Å]	H•••A [Å]	D–A [Å]	D–H•••A[°]
1				
C(1)–H(1)•••Cl(1)	0.93	2.82	3.372(11)	118.8
C(1)–H(1)•••F(9)[a]	0.93	2.38	3.106(11)	135.2
C(2)–H(2)•••F(12)[a]	0.93	2.38	3.025(10)	126.2
C(13)–H(13)•••F(9)[b]	0.93	2.53	3.308(12)	141.6
C(22)–H(22B)•••F(6)[c]	0.96	2.45	3.274(13)	143.5
C(23)–H(23B)•••F(7)[a]	0.96	2.44	3.29(2)	147.1
2				
C(1)–H(1)•••Cl(1)	0.93	2.81	3.354(8)	118.8
C(1)–H(1)•••F(10)[d]	0.93	2.34	3.232(10)	160.4
C(4)–H(4)•••F(6)[e]	0.93	2.53	3.087(10)	118.4
C(9)–H(9)•••F(9)	0.93	2.49	3.395(9)	164.7
C(12)–H(12)•••F(7)	0.93	2.39	3.231(10)	149.9
C(14)–H(14)•••F(11)[f]	0.93	2.53	3.103(10)	120.4
C(15)–H(15)•••Cl(1)	0.93	2.83	3.387(8)	119.8
C(15)–H(15)•••F(1)	0.93	2.55	3.304(9)	138.4
C(23)–H(23)•••F(12)[g]	0.93	2.51	3.277(10)	140.2
C(21)–H(21)•••F(3)[h]	0.93	2.48	3.402(11)	174.5
3				
C(4)–H(4)•••N(4)[i]	0.93	2.62	3.548(9)	173.0
C(12)–H(12)•••N(4)[i]	0.93	2.56	3.486(10)	175.0
4				
C(7)–H(7)•••Cl(1)[a]	0.93	2.80	3.329(8)	116.8
C(12)–H(12)•••O(3)[j]	0.93	2.45	3.236(11)	142.9
C(21)–H(21)•••O(1)	0.93	2.36	2.682(10)	100.0
6				
C(4)–H(4)•••Cl(2)[f]	0.93	2.66	3.570(3)	165.0
C(7)–H(7)•••Cl(2)[f]	0.93	2.82	3.661(3)	150.6
C(12)–H(12)•••N(4)	0.93	2.62	3.380(7)	139.2
C(13)–H(13)•••Cl(2)[k]	0.93	2.64	3.489(3)	151.6
C(17)–H(17)•••Cl(2)[f]	0.93	2.70	3.561(3)	154.6
C(21)–H(21)•••O(1)	0.93	2.38	3.712(4)	100.9
C(28)–H(28A)•••Cl(1)[k]	0.96	2.80	3.679(6)	152.5

Symmetry codes: (a) = x,1/2-y,-1/2+z; (b) = -x,-y,2-z; (c) = 1-x,-1-y,2-z; (d) = x,1/2-y,1/2+z; (e) = -1+x,1/2-y,-1/2+z; (f) = 1-x,-y,1-z; (g) = -x,1/2+y,1/2-z; (h) = -1+x,y,-1+z; (i) = 1+x,y,z; (j) = -1+x,y,z, (k) = -x,1-y,1-z

Table S2. Short π•••π interactions for the complexes.

Cg(I)•••Cg(J)	Cg(I)•••Cg(J) [Å]	α[°]	β[°]	γ [°]	Cg(I)-Perp [Å]	Cg(J)-Perp [Å]
1						
Cg(1)•••Cg(1)[c]	3.867(5)	0	24.57	24.57	-3.517(4)	-3.516(4)
4						
Cg(2)•••Cg(3)[d]	3.912 (5)	7.3(4)	26.43	26.91	3.488(4)	3.503(3)
Cg(4)•••Cg(5)[l]	3.941(4)	3.3(4)	26.25	28.73	-3.456(3)	-3.534(3)
Cg(3)•••Cg(3)[m]	3.684(4)	0	21.02	21.02	-3.439(3)	-3.439(3)
6						
Cg(2)•••Cg(4)[f]	3.9083(17)	7.02(14)	25.82	18.96	-3.6963(12)	-3.5182(11)
Cg(5)•••Cg(5)[k]	3.5655(17)	0	21.33	21.33	-3.3213(12)	-3.3213(12)
Cg(5)•••Cg(5)[n]	3.7138(17)	0	24.25	24.25	3.3861(12)	3.3860(12)

α = dihedral angle between *Cg*(I) and *Cg*(J); *Cg*(I)-Perp = Perpendicular distance of *Cg*(I) on ring J; *Cg*(J)-Perp = perpendicular distance of *Cg*(J) on ring I; β = angle *Cg*(I)→*Cg*(J) vector and normal to ring I; γ = angle *Cg*(I) →*Cg*(J) vector and normal to plane J;

Cg1 is the centroid of atoms C(16)/C(17)/C(18)/C(19)/C(20)/C(21); Cg2 is the centroid of atoms N(1)/C(1)/C(2)/C(3)/C(4)/C(5); Cg3 is the centroid of atoms C(20)/C(21)/C(22)/C(23)/C(24)/C(25); Cg4 is the centroid of atoms N(2)/C(6)/C(7)/C(8)/C(9)/C(10); Cg5 is the centroid of atoms N(3)/C(11)/C(12)/C(13)/C(14)/C(15);

Symmetry codes: (c) = 1-*x*,-1-*y*,2-*z*; (d) = *x*,1/2-*y*,1/2+*z*; (f) = 1-*x*,-*y*,1-*z*; (k) = -*x*,1-*y*,1-*z*, (l) = -*x*,-*y*,-*z*; (m) = -*x*,-*y*,-1-*z*; (n) = 1-*x*,1-*y*,1-*z*;

Table S3. X—Y•••Cg(J)(π-ring) interactions for the complexes.

Y-X(I)•••Cg(J)	X(I)•••Cg(J) [Å]	X-Perp [Å]	γ [°]	Y-X(I)•••Cg(J) [°]
1				
Au(1)-Cl(1)•••Cg(5)[o]	3.835(4)	-3.365	28.65	174.38(12)
P(1)-F(6)•••Cg(4)[p]	3.328(8)	-3.041	23.95	124.8(5)
2				
Au(1)-Cl(1)•••Cg(1)[q]	3.834(3)	-3.375	28.32	114.83(7)
P(1)-F(2)•••Cg(2)[d]	3.189(8)	2.920	23.68	155.2(5)
P(1)-F(4)•••Cg(4)[d]	3.337(8)	3.222	15.11	124.1(4)
P(2)-F(8)•••Cg(5)[r]	3.415(9)	-3.317	13.81	124.5(4)
3				
C(13)-H(13)•••Cg(6)[s]	2.96	-2.91	10.33	136.00
Pt(2)-Cl(1)•••Cg(2)[t]	3.795(3)	-3.439	25.02	111.71(6)
Pt(2)-Cl(1)•••Cg(5)[u]	3.837(3)	3.578	21.15	69.93(5)
6				
Cu(1)-Cl(2)•••Cg(2)[j]	3.8024(14)	3.795	3.63	174.33(3)

γ = angle X(I)→Cg(J) vector and normal to plane J.

Cg1 is the centroid of atoms C(16)/C(17)/C(18)/C(19)/C(20)/C(21); Cg2 is the centroid of atoms N(1)/C(1)/C(2)/C(3)/C(4)/C(5); Cg4 is the centroid of atoms N(2)/C(6)/C(7)/C(8)/C(9)/C(10); Cg5 is the centroid of atoms N(3)/C(11)/C(12)/C(13)/C(14)/C(15); Cg6 is the centroid of atoms C(35)/C(36)/C(37)/C(38)/C(39)/C(40);

Symmetry codes: (d) = *x*,1/2-*y*,1/2+*z*; (j) = -1+x,y,z, (o) = -*x*,1/2+*y*,3/2-*z*; (p) = *x*,*y*,*z*; (q) = 1+*x*,1/2-*y*,1/2+*z*; (r) = -*x*,-*y*,1-*z*; (s) = 2-*x*,-*y*,1-*z*; (t) = 1-*x*,1-*y*,-*z*; (u) = 2-*x*,1-*y*,-*z*

Table S4. The energies and characters of the selected spin-allowed electronic transitions for **1** calculated with the TDDFT/PBE1PBE method, together with assignment to the experimental absorption bands. UV-Vis absorption spectrum of **1** was recorded in CH_3CN solution ($c = 5 \cdot 10^{-5}$ M).

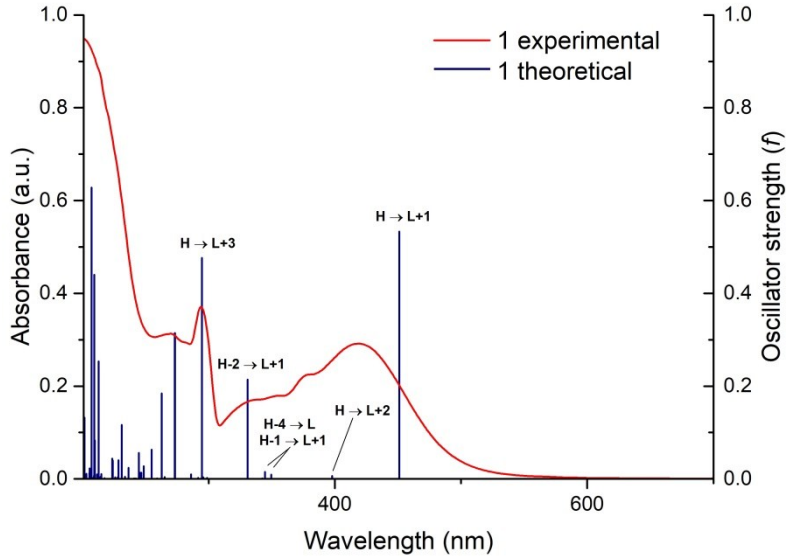

Experimental absorption λ; nm (10^4 ε; M^{-1} cm^{-1})	Calculated transitions				
	Major contribution (%)	Character	E [eV]	λ [nm]	Oscillator strength
419 (1.72)	H → L (98%)	LMCT	2.43	509.45	*0.0004* S_1
	H → L+1 (99%)	ILCT	2.75	450.94	*0.5333* S_2
382(1.33)	H → L+2 (97%)	ILCT	3.12	397.93	*0.0066* S_3
353 (1.06)	H-4 → L (66%) H-1 → L+1 (21%)	LMCT ILCT	3.55	349.69	*0.0094* S_6
	H-1 → L+1 (71%) H-4 → L (22%)	ILCT LMCT	3.60	344.69	*0.0152* S_7
	H-2 → L+1 (85%)	LE	3.75	330.80	*0.2141* S_9
296 (2.52)	H → L+3 (67%)	ILCT	4.21	294.76	*0.4768* S_{12}
287 (1.84)	H → L+4 (96%)	ILCT	4.25	291.40	*0.0022* S_{13}
	H-3 → L+1 (82%)	LLCT	4.33	286.18	*0.0099* S_{14}
275 (1.84)	H-2 → L+2 (76%)	LE	4.54	273.29	*0.3147* S_{17}
264 (1.86)	H → L+5 (73%) H-5 → L+1 (17%)	ILCT LE	4.72	262.89	*0.1846* S_{19}
	H-2 → L+3 (36%) H-5 → L+2 (19%)	LE LE	5.36	231.28	*0.1164* S_{30}
	H-1 → L+5 (28%) H-13 → L (17%) H-10→ L+1 (12%)	ILCT LMCT LE	5.82	212.88	*0.2538* S_{41}
	H-2 → L+5 (50%)	LE	5.92	209.46	*0.4401* S_{44}
	H-11 → L (33%) H-7 → L+2 (14%) H-12 → L (12%) H-3 → L+3 (12%)	LE LE LE LLCT	5.98	207.31	*0.6283* S_{48}
	H-8 → L+2 (31%) H → L+8 (14%) H-5 → L+4 (12%) H-9 → L+2 (12%)	ILCT ILCT LE LE	6.15	201.73	*0.1325* S_{53}

LE (locally excited) = $\pi_{terpy} \rightarrow \pi^*_{terpy}$; ILCT (intraligand charge transfer) = $\pi_R \rightarrow \pi^*_{terpy}$

Table S5. The energies and characters of the selected spin-allowed electronic transitions for **2** calculated with the TDDFT/PBE1PBE method, together with assignment to the experimental absorption bands. UV-Vis absorption spectrum of **2** was recorded in CH_3CN solution ($c = 5 \cdot 10^{-5}$ M).

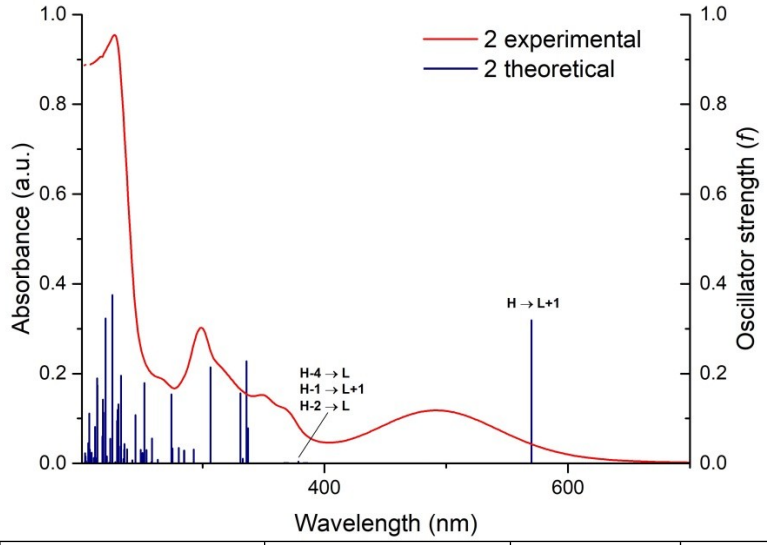

Experimental absorption λ; nm (10^4 ε; M^{-1} cm^{-1})	Major contribution (%)	Character	E [eV]	λ [nm]	Oscillator strength
493 (0.76)	H → L+1 (99%)	ILCT	2.17	570.07	*0.3190* S_2
367 (0.78)	H-4 → L (76%)	LMCT	3.22	384.51	*0.0005* S_6
	H-1 → L+1 (98%)	ILCT	3.27	378.62	*0.0041* S_7
	H-5 → L (95%)	LMCT	3.36	368.68	*0.0008* S_8
	H-2 → L (77%)	LMCT	3.38	367.05	*0.0013* S_9
347 (0.99)	H-3 → L+1 (46%) H → L+4 (43%)	LE ILCT	3.69	335.97	*0.2279* S_{11}
	H-2 → L+1 (49%) H-3 → L+1 (22%) H → L+4 (16%)	ILCT LE ILCT	3.74	331.14	*0.1567* S_{13}
298 (2.07)	H → L+5 (91%)	ILCT/LE	4.04	306.62	*0.2146* S_{16}
	H-3 → L+2 (49%) H-4 → L+1 (21%) H → L+6 (11%)	LE LLCT LE	4.52	274.54	*0.1542* S_{23}
263 (1.25)	H-7 → L+1 (70%)	LC/LLCT	4.91	252.24	*0.1794* S_{29}
	H-9 → L+1 (63%)	LE	5.06	244.89	*0.1080* S_{33}
	H-6 → L+2 (48%) H → L+8 (9%)	LE ILCT	5.32	233.04	*0.1957* S_{41}
	H-7 → L+2 (48%) H-3 → L+4 (15%) H-10 → L+1 (9%)	LC/LLCT LE ILCT	5.49	225.97	*0.3755* S_{47}
	H-17 → L (29%) H-11→ L+1 (12%) H-15 → L (10%)	*d* → *d* LE LMCT	5.62	220.51	*0.3230* S_{51}

Table S6. The energies and characters of the selected spin-allowed electronic transitions for **3** calculated with the TDDFT/PBE1PBE method, together with assignment to the experimental absorption bands. UV-Vis absorption spectrum of **3** was recorded in CH_3CN solution ($c = 5 \cdot 10^{-5}$ M).

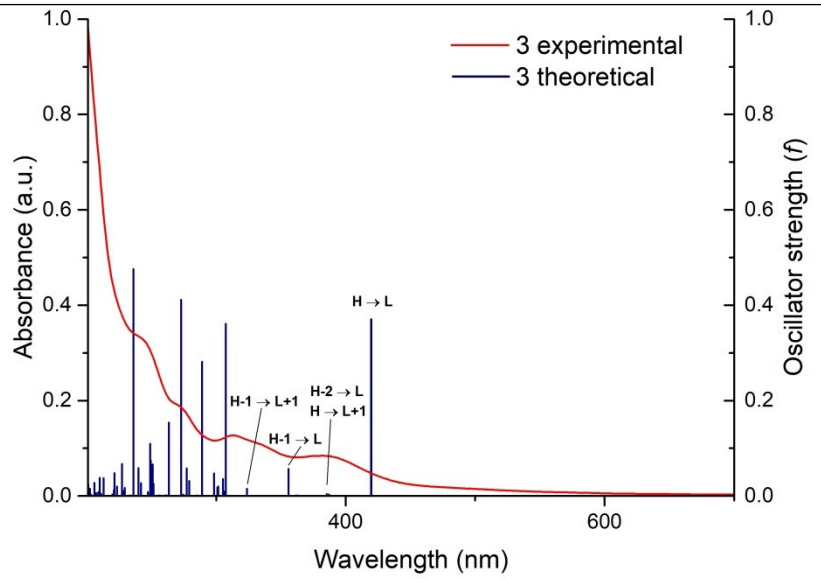

Experimental absorption λ; nm (10^4 ε; M^{-1} cm^{-1})	Major contribution (%)	Character	E [eV]	λ [nm]	Oscillator strength
378 (0.38)	H → L (94%)	ILCT/MLCT	2.95	419.70	*0.3705* S_1
	H-2 → L (98%)	MLCT	3.20	387.06	*0.0035* S_2
	H→ L+1 (93%)	ILCT/MLCT	3.22	385.31	*0.0044* S_3
	H-3 → L (89%)	MLCT	3.42	362.34	*0.0008* S_4
	H-1 → L (89%)	MLCT	3.48	355.86	*0.057* S_5
312 (0.57)	H-1 → L+1 (90%)	MLCT	3.83	323.84	*0.0156* S_8
	H-6 → L (77%) H-5 → L (13%)	LE/MLCT ILCT	4.03	307.36	*0.3611* S_9
270 (0.85)	H → L+2 (91%)	ILCT/MLCT	4.29	289.17	*0.2819* S_{15}
	H-6 → L+1 (66%) H-3 → L+1 (9%) H → L+4 (9%)	LE/MLCT LE/MLCT MLCT	4.54	272.94	*0.4116* S_{20}
	H → L+4 (78%) H-6 → L+1 (9%)	ILCT/MLCT LE/MLCT	4.70	263.49	*0.1543* S_{21}
	H-3 → L+2 (22%) H → L+6 (40%) H-1 → L+3 (7%) H-5 → L+4 (6%)	ILCT/MLCT LE/MLCT MLCT ILCT	4.98	248.98	*0.1096* S_{28}
	H-7 → L+1 (81%) H-3 → L+2 (15%)	LE LE/MLCT	5.25	236.21	*0.4762* S_{34}

Table S7. The energies and characters of the selected spin-allowed electronic transitions for **4** calculated with the TDDFT/PBE1PBE method, together with assignment to the experimental absorption bands. UV-Vis absorption spectrum of **4** was recorded in CH_3CN solution ($c = 5 \cdot 10^{-5}$ M).

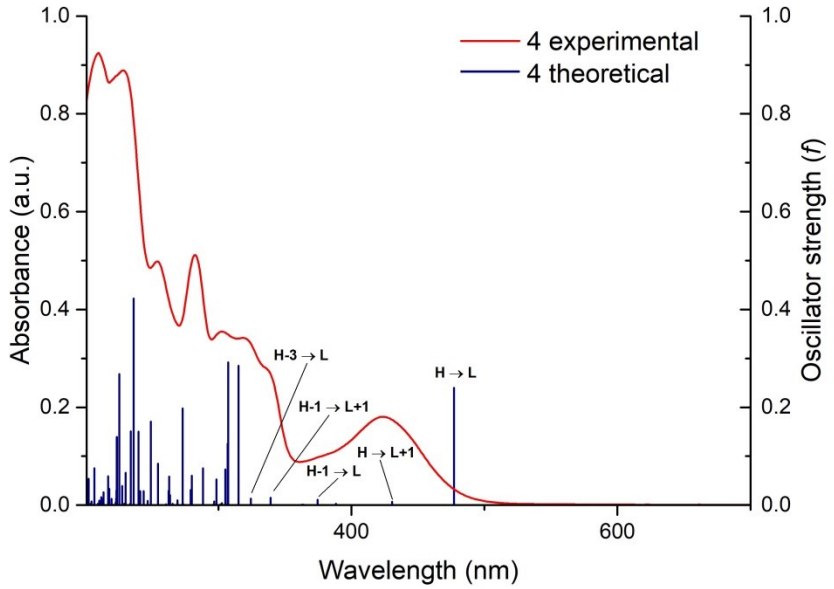

Experimental absorption λ; nm (10^4 ε; M^{-1} cm^{-1})	Major contribution (%)	Character	E [eV]	λ [nm]	Oscillator strength
423 (0.85)	H → L (99%)	ILCT	2.60	477.10	*0.2403* S_1
	H → L+1 (98%)	ILCT	2.88	430.59	*0.0074* S_2
	H-2 → L (97%)	MLCT	3.19	388.36	*0.003* S_3
	H-1 → L (93%)	MLCT	3.31	374.58	*0.0115* S_4
338 (1.33)	H-1 → L+1 (95%)	MLCT	3.66	339.36	*0.0151* S_7
	H-3 → L (91%)	ILCT	3.82	324.45	*0.0138* S_9
315 (1.62)	H → L+2 (86%) H → L+4 (7%)	ILCT LE/ILCT	3.94	315.22	*0.2849* S_{10}
302 (1.71)	H-6 → L (34%) H-1 → L+5 (7%)	ILCT/LE/MLCT *d→d/MLCT*	4.04	307.45	*0.2924* S_{11}
	H-4→ L+1 (23%) H-1→ L+5 (16%) H-5 → L+1 (15%)	MLCT/LE *d→d*/MLCT MLCT/ILCT	4.04	307.01	*0.126* S_{12}
283 (2.67)	H-6 → L+1 (46%)	ILCT/LE/MLCT	4.54	273.15	*0.1981* S_{23}
253 (2.4)	H-4 → L+2 (70%)	MLCT/LE	4.98	249.34	*0.1712* S_{32}
	H-4 → L+3 (33%) H-9 → L (22%) H-1 → L+4 (17%)	MLCT/LE ILCT/LE MLCT	5.17	240.00	*0.1504* S_{37}
	H-8 → L+1 (80%) H-4 → L+2 (15%)	LE MLCT/LE	5.25	236.45	*0.4226* S_{38}
	H-3 → L+2 (79%) H → L+7 (8%)	ILCT LE	5.30	234.26	*0.1514* S_{39}
	H-3 → L+4 (44%) H → L+7 (9%) H-6 → L+2 (8%)	LE/ILCT LE ILCT/LE/MLCT	5.50	225.64	*0.2682* S_{46}

Table S8. Comparison of ^{1}H NMR chemical shifts of **1-4** and ligands L^1 and L^2.

compound (medium)	proton chemical shift (ppm)											
	A1	**A2**	**A3**	**A4**	**B2**	**C2**	**C3**					**C5**
1 (CD_3CN)	9.16	8.10	8.73 – 8.69	8.73 – 8.69	8.73 – 8.69	8.16	7.28					3.97
3 (CD_3SOCD_3)	8.76 – 8.72	7.84	8.44	8.76 – 8.72	8.80	8.14	7.21 – 7.15					3.92
L^1 (CD_3CN)	8.72	7.47 – 7.41	7.96	8.67	8.70	7.86	7.11					3.87
L^1 (CD_3SOCD_3)	8.76	7.54 – 7.48	8.03	8.66	8.67	7.89	7.14					3.85
	A1	**A2**	**A3**	**A4**	**B2**	**C2**	**C3**	**C6**	**C7**	**C8**	**C9**	**C11**
2 (CD_3CN)	9.19	8.14 – 8.07	8.67	8.60	8.71	7.84	7.23	8.14 – 8.07	7.74 – 7.70	7.74 – 7.70	8.46 – 8.43	4.15
4 (CD_3SOCD_3)	8.84	7.89	8.44	8.70	8.82	7.73	7.23	8.04 – 8.00	7.68 – 7.64	7.68 – 7.64	8.37 – 8.34	4.10
L^2 (CD_3CN)	8.68	7.47 – 7.41	8.03 – 7.95	8.74	8.57	7.62 – 7.52	7.08	8.03 – 7.95	7.62 – 7.52	7.62 – 7.52	8.36	4.08
L^2 (CD_3SOCD_3)	8.75 – 8.70	7.54 – 7.49	8.05	8.75 – 8.70	8.53	7.64 – 7.57	7.15	7.94 – 7.90	7.64 – 7.57	7.64 – 7.57	8.33 – 8.30	4.06

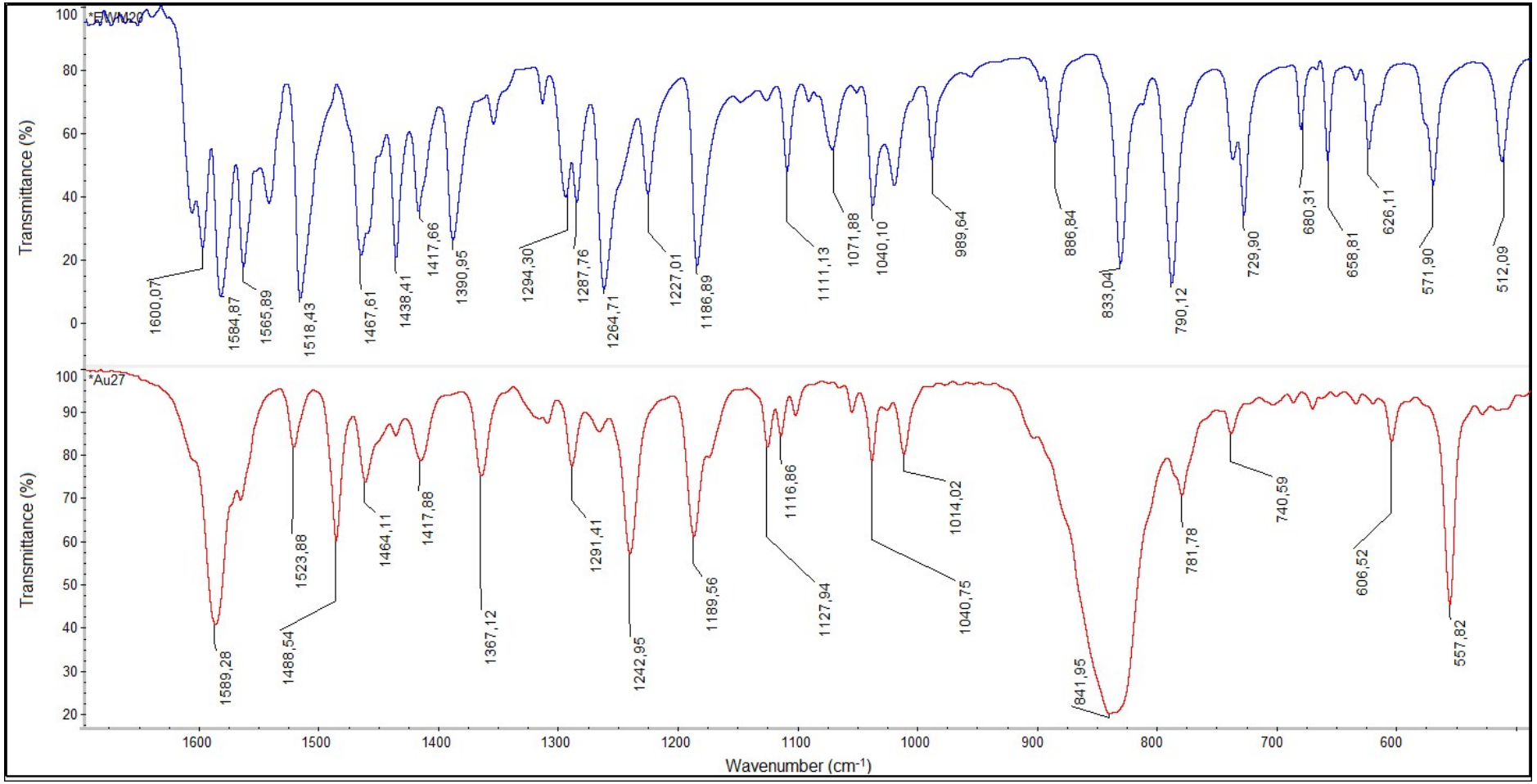
*Au27
Transmittance (%)
Wavenumber (cm-1)
1600,07
1584,87
1565,89
1518,43
1467,61
1438,41
1417,66
1390,95
1294,30
1287,76
1264,71
1227,01
1186,89
1111,13
1071,88
1040,10
989,64
886,84
833,04
790,12
729,90
680,31
658,81
626,11
571,90
512,09
1589,28
1488,54
1523,88
1464,11
1417,88
1367,12
1291,41
1242,95
1189,56
1127,94
1116,86
1040,75
1014,02
841,95
781,78
740,59
606,52
557,82

(a)

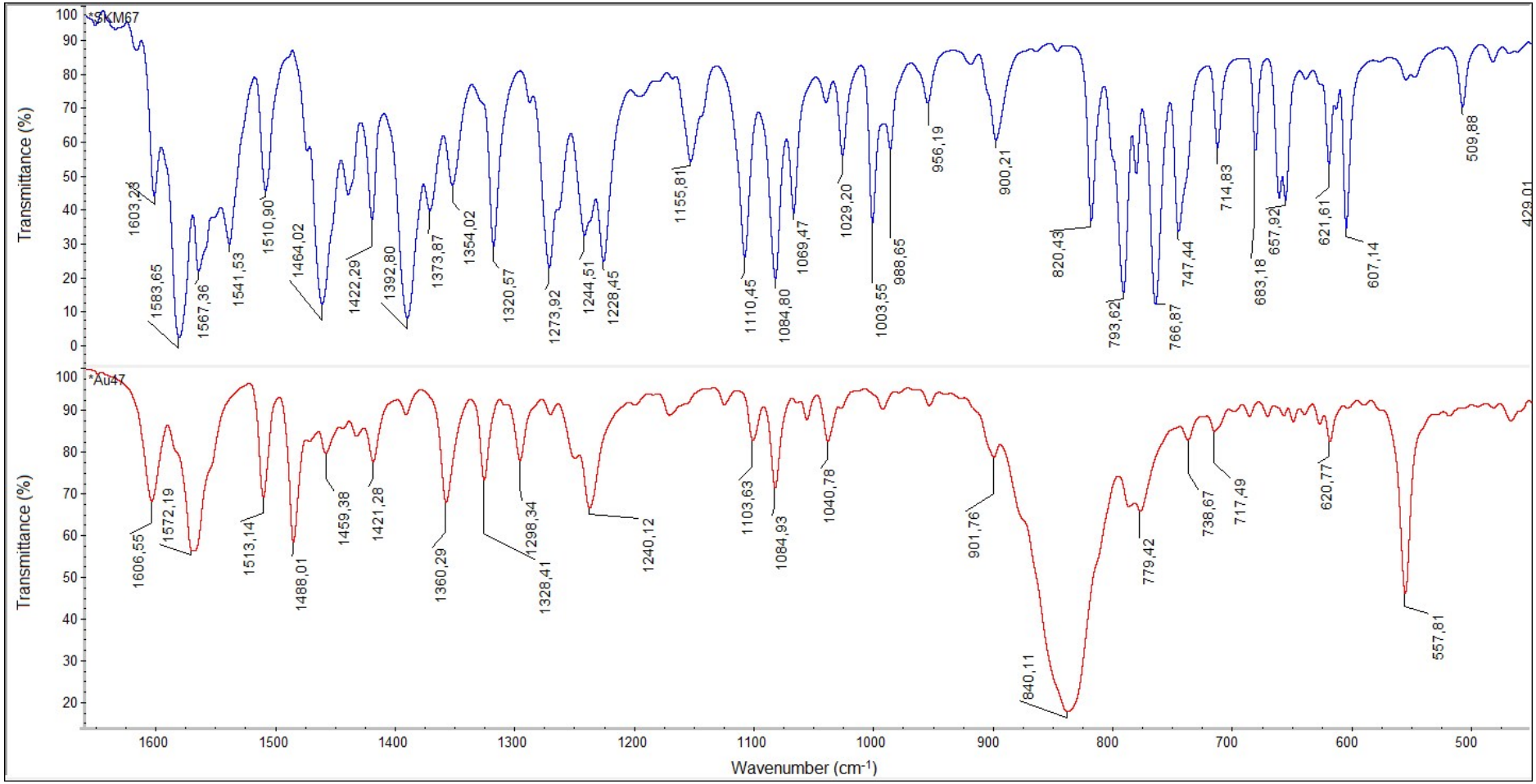
*SKM67
Transmittance (%)
1603,28
1583,65
1567,36
1541,53
1510,90
1464,02
1422,29
1392,80
1373,87
1354,02
1320,57
1273,92
1244,51
1228,45
1155,81
1110,45
1084,80
1069,47
1029,20
1003,55
988,65
956,19
900,21
820,43
793,62
766,87
747,44
714,83
683,18
657,92
621,61
607,14
509,88
429,01
*Au47
1606,55
1572,19
1513,14
1488,01
1459,38
1421,28
1360,29
1328,41
1298,34
1240,12
1103,63
1084,93
1040,78
901,76
840,11
779,42
738,67
717,49
620,77
557,81
Wavenumber (cm-1)

(b)

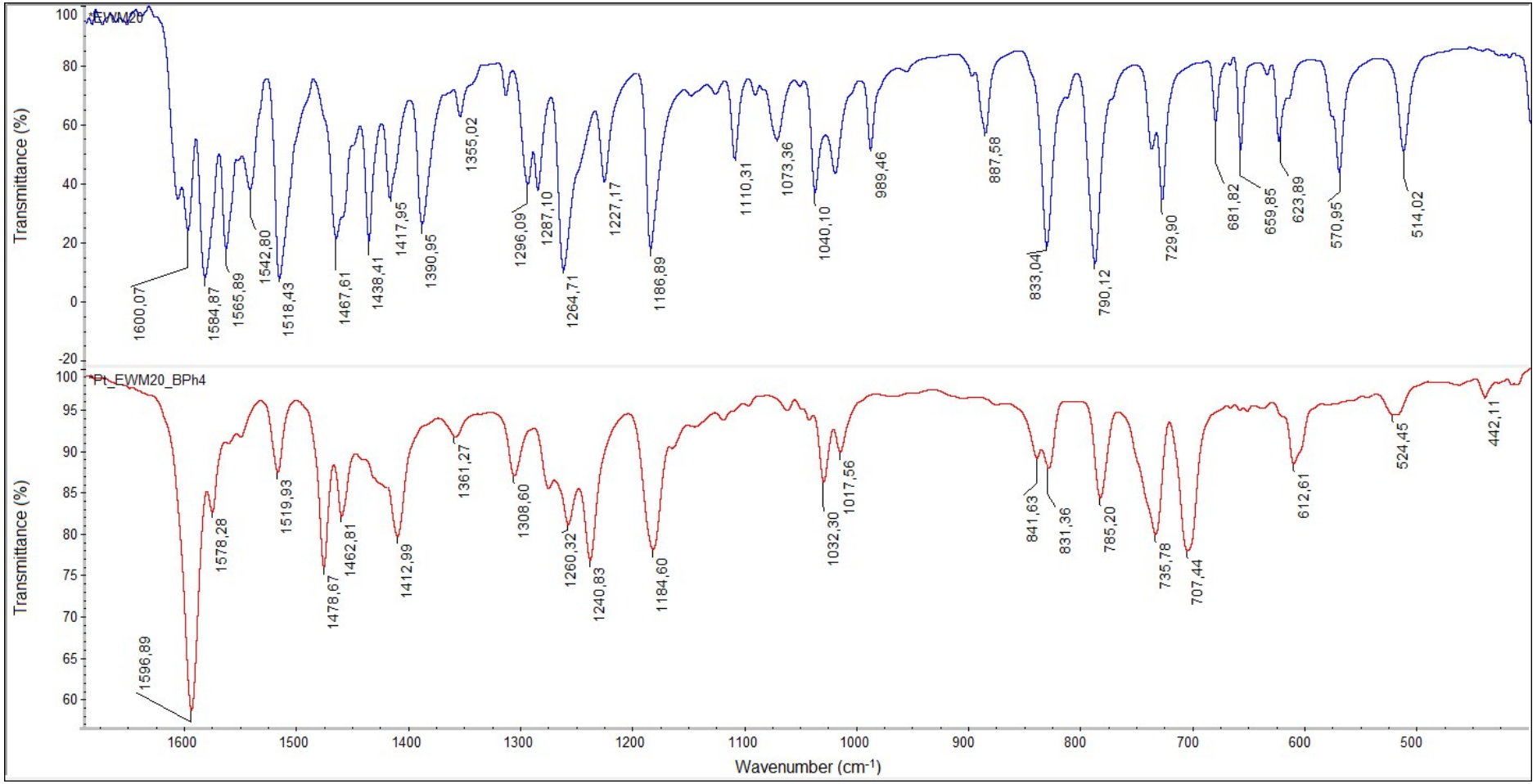
EWM20
Transmittance (%)
1600,07
1584,87
1565,89
1542,80
1518,43
1467,61
1438,41
1417,95
1390,95
1355,02
1296,09
1287,10
1264,71
1227,17
1186,89
1110,31
1073,36
1040,10
989,46
887,58
833,04
790,12
729,90
681,82
659,85
623,89
570,95
514,02
Pt_EWM20_BPh4
Transmittance (%)
1596,89
1578,28
1519,93
1478,67
1462,81
1412,99
1361,27
1308,60
1260,32
1240,83
1184,60
1032,30
1017,56
841,63
831,36
785,20
735,78
707,44
612,61
524,45
442,11
Wavenumber (cm-1)

(c)

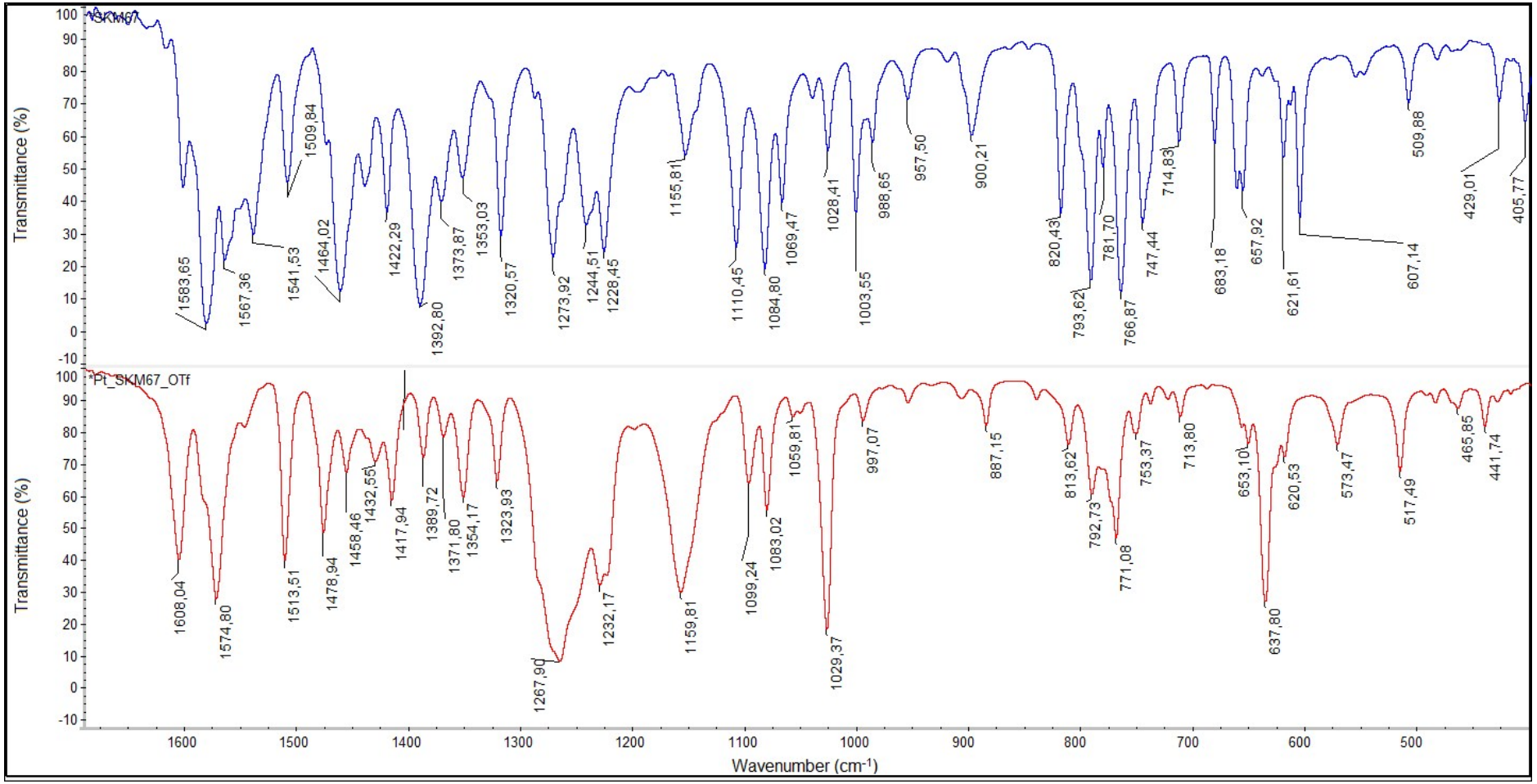
SKM67
Transmittance (%)
1583,65
1567,36
1541,53
1509,84
1464,02
1422,29
1392,80
1373,87
1353,03
1320,57
1273,92
1244,51
1228,45
1155,81
1110,45
1084,80
1069,47
1028,41
1003,55
988,65
957,50
900,21
820,43
793,62
781,70
766,87
747,44
714,83
683,18
657,92
621,61
607,14
509,88
429,01
405,77
Pt_SKM67_OTf
Transmittance (%)
1608,04
1574,80
1513,51
1478,94
1458,46
1432,55
1417,94
1389,72
1371,80
1354,17
1323,93
1267,90
1232,17
1159,81
1099,24
1083,02
1059,81
1029,37
997,07
887,15
813,62
792,73
771,08
753,37
713,80
653,10
637,80
620,53
573,47
517,49
465,85
441,74
Wavenumber (cm-1)

(d)

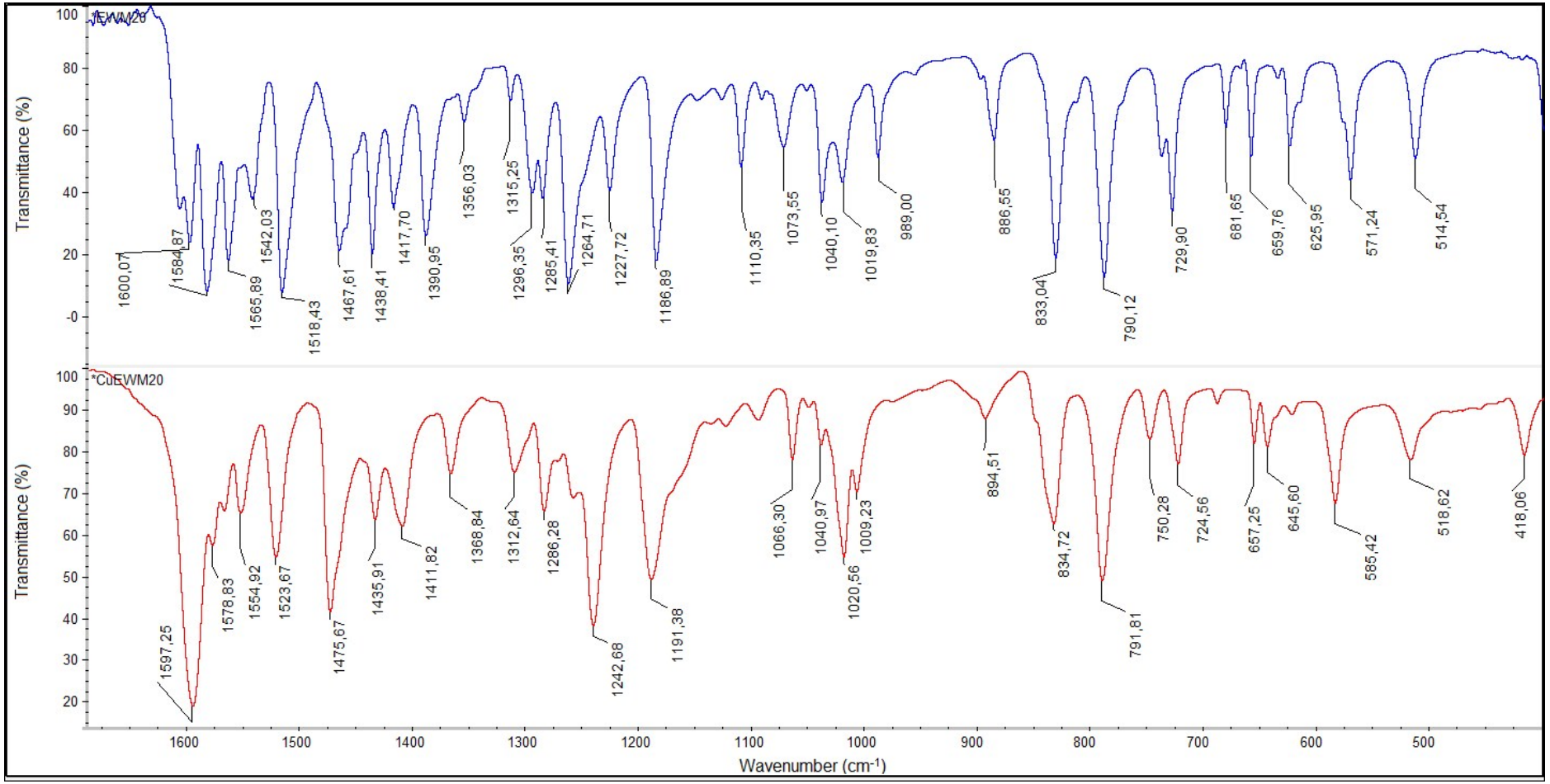
JEWM20
Transmittance (%)
1600,07
1584,87
1565,89
1542,03
1518,43
1467,61
1438,41
1417,70
1390,95
1356,03
1315,25
1296,35
1285,41
1264,71
1227,72
1186,89
1110,35
1073,55
1040,10
1019,83
989,00
886,55
833,04
790,12
729,90
681,65
659,76
625,95
571,24
514,54
*CuEWM20
Transmittance (%)
1597,25
1578,83
1554,92
1523,67
1475,67
1435,91
1411,82
1368,84
1312,64
1286,28
1242,68
1191,38
1066,30
1040,97
1020,56
1009,23
894,51
834,72
791,81
750,28
724,56
657,25
645,60
585,42
518,62
418,06
Wavenumber (cm-1)

(e)

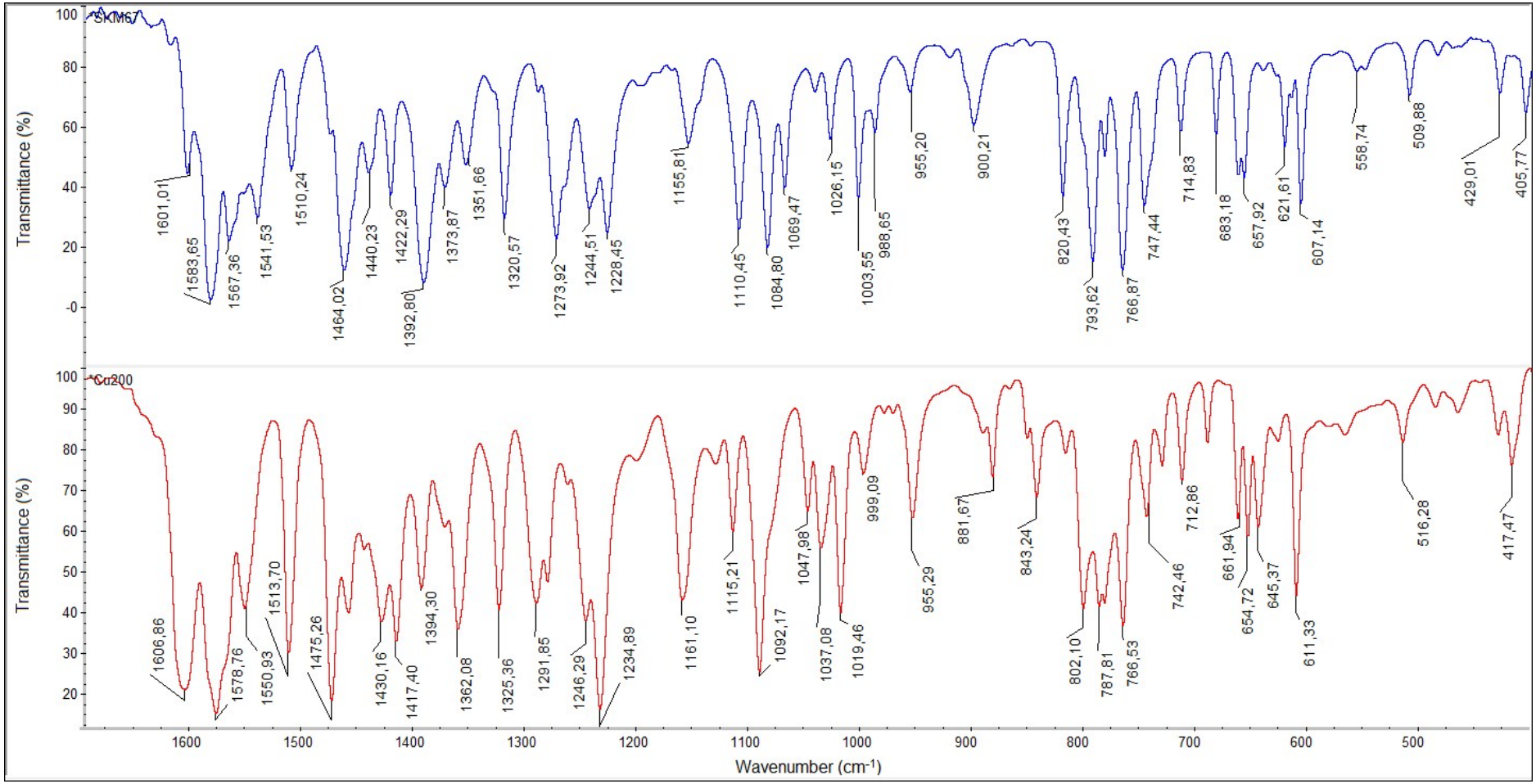

(f)

Figure S1. IR spectra of the free ligands L^1 or L^2 (blue) and complexes **1-6** (red) (a-f).

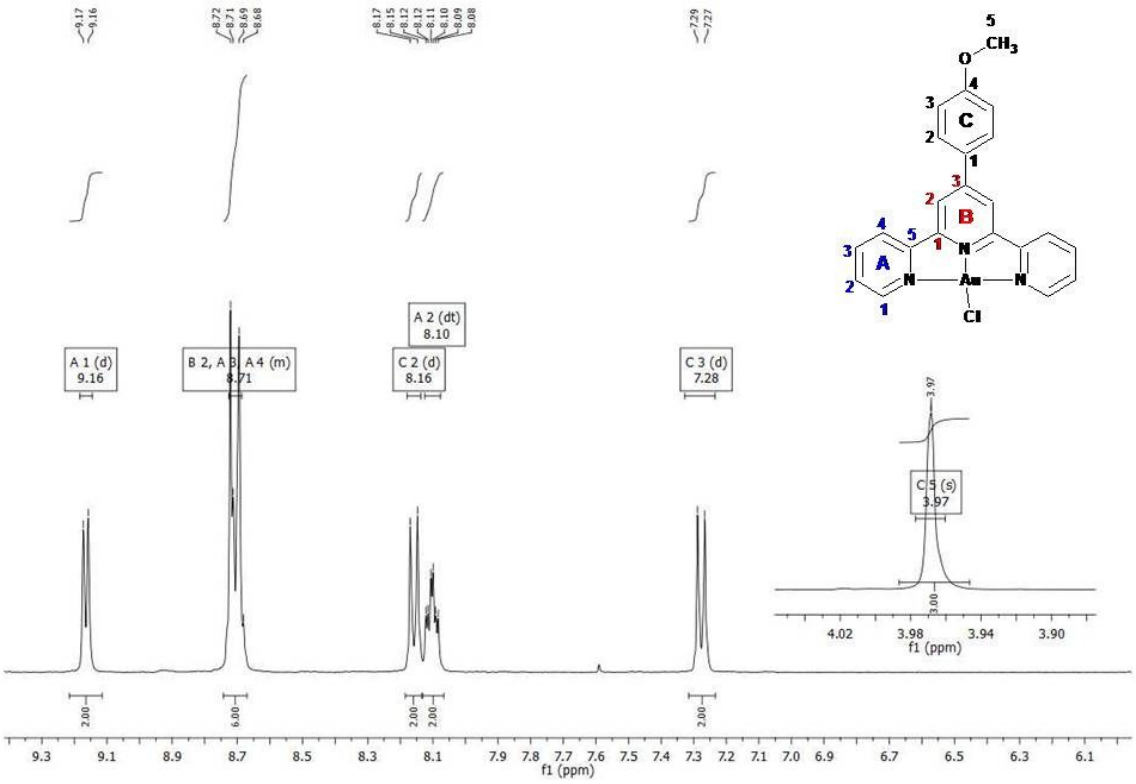
A 1 (d)
9.16
B 2, A 3, A 4 (m)
8.71
A 2 (dt)
8.10
C 2 (d)
8.16
C 3 (d)
7.28
C 5 (s)
3.97
f1 (ppm)

(a)

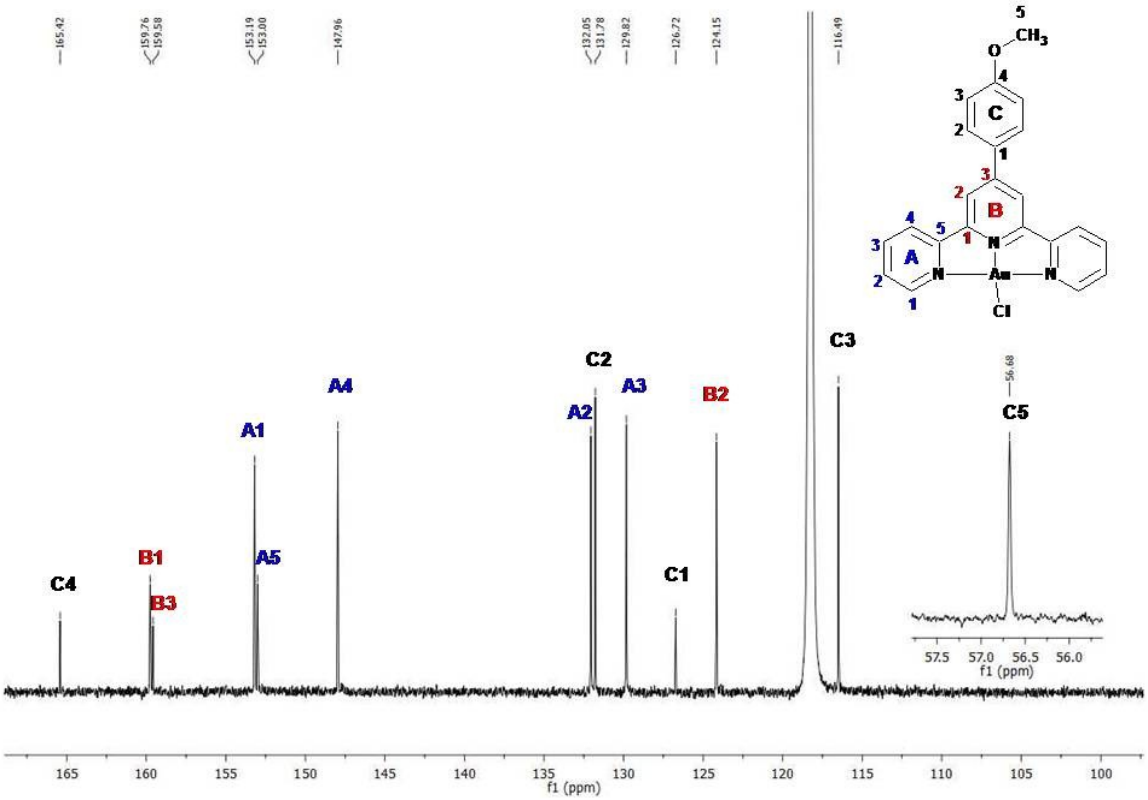
C4
B1
B3
A1
A5
A4
A2
C2
A3
C1
B2
C3
C5
f1 (ppm)

(b)

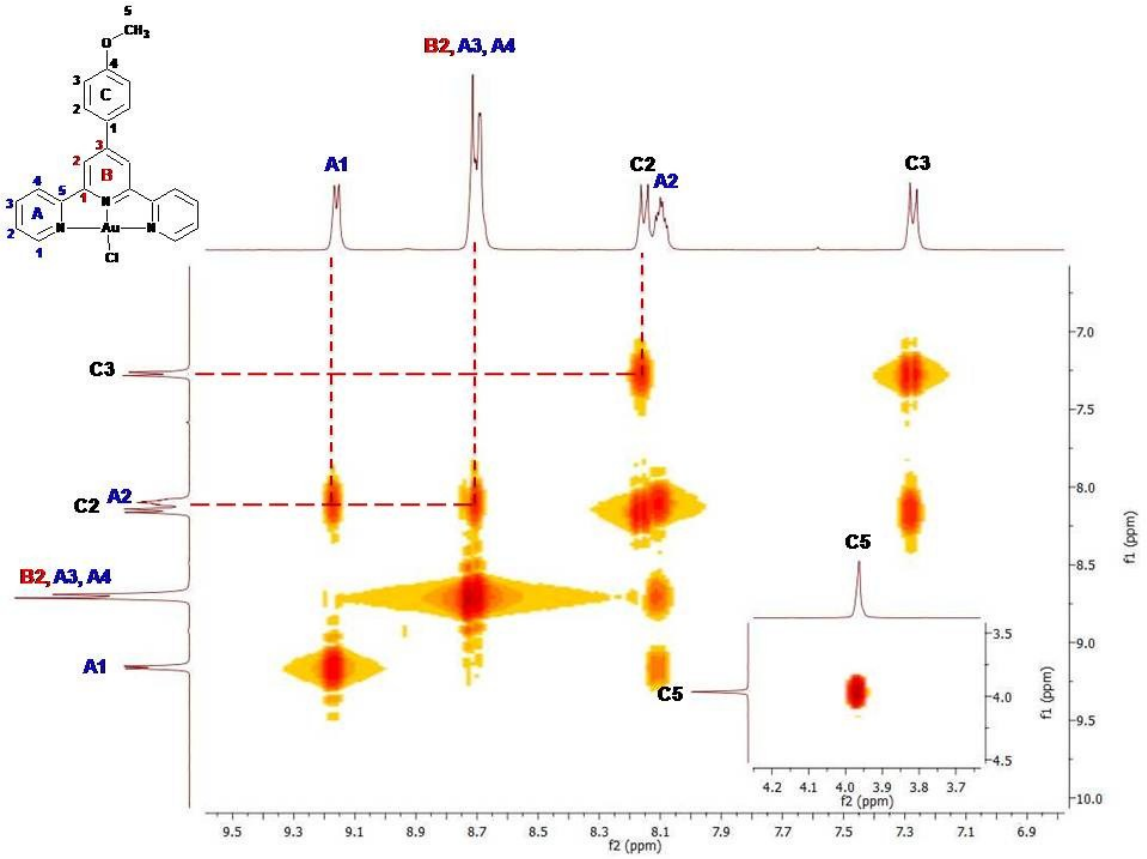
B2, A3, A4
A1
C2
A2
C3
C5
f2 (ppm)
f1 (ppm)

(c)

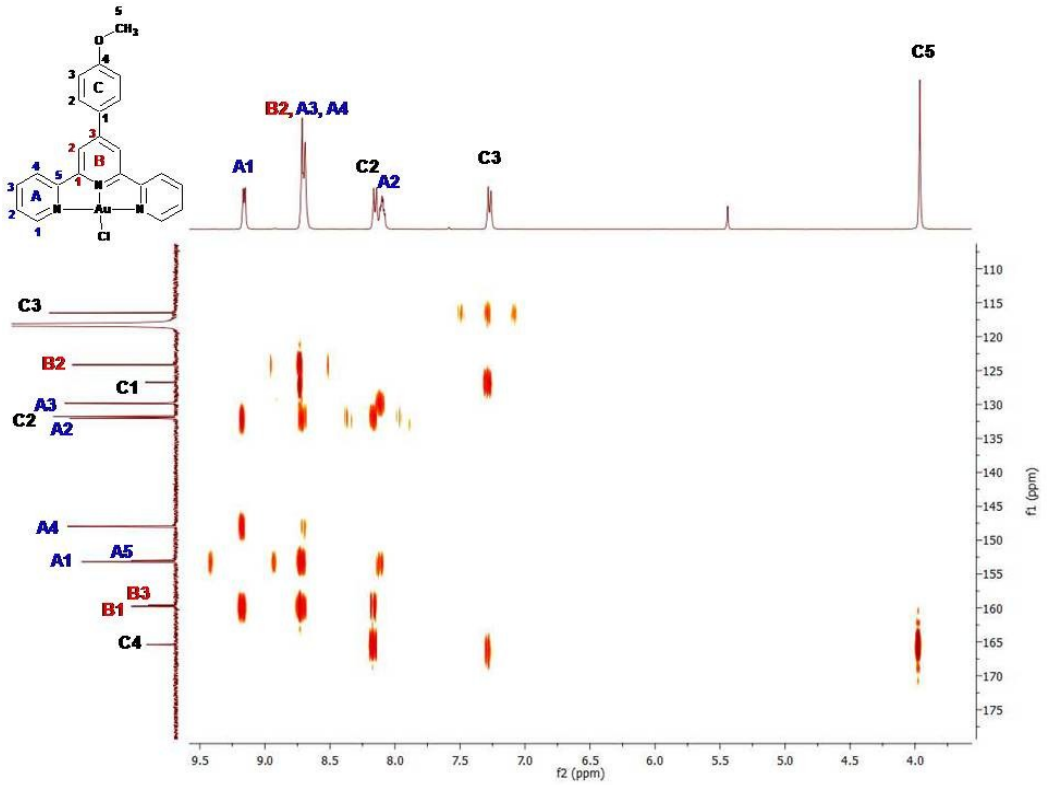
C5
B2, A3, A4
A1
C2
A2
C3
B2
C1
A3
A4
A5
B3
B1
C4
f2 (ppm)
f1 (ppm)

(d)

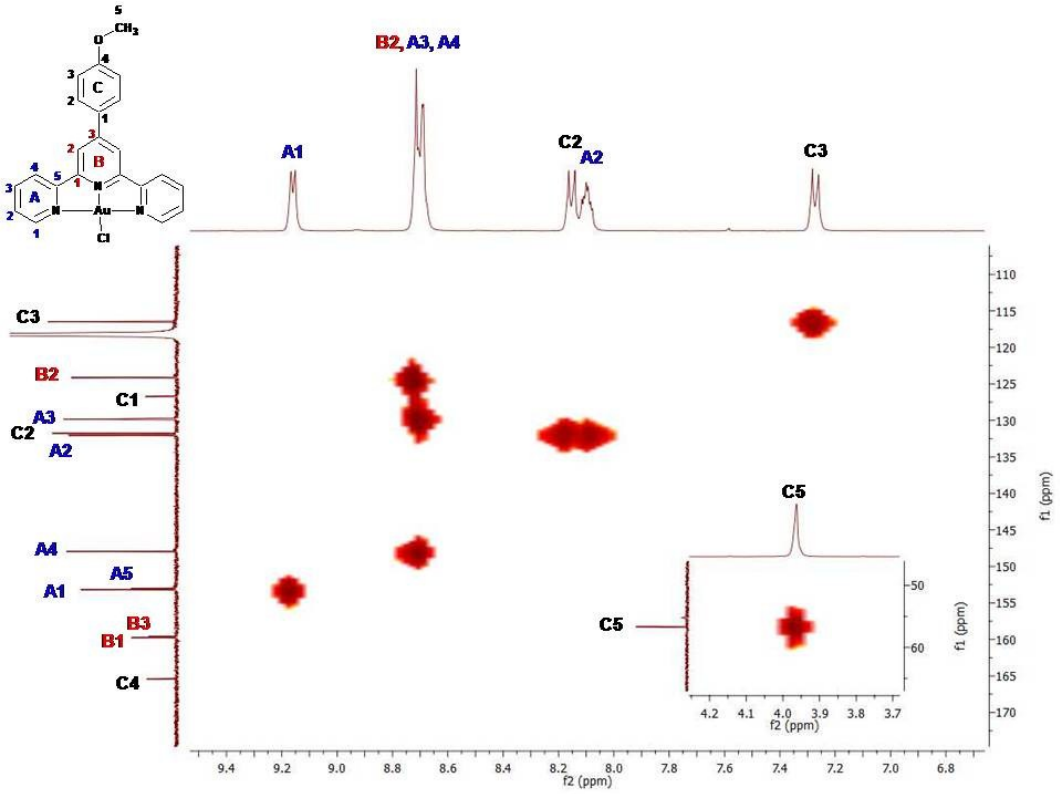

(e)

Figure S2. ^{1}H NMR (a), ^{13}C NMR (b), COSY (c), HMBC (d) and HMQC (e) NMR of **1**

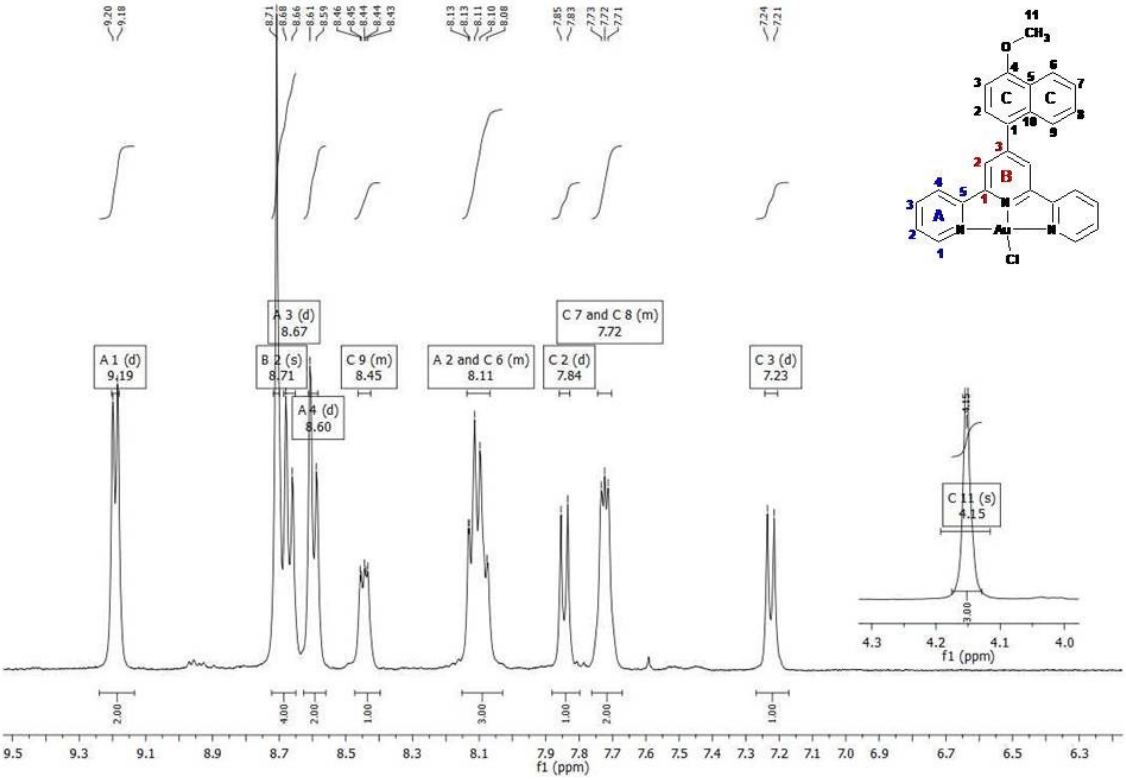
A 1 (d)
9.19
B 2 (s)
8.71
A 3 (d)
8.67
A 4 (d)
8.60
C 9 (m)
8.45
A 2 and C 6 (m)
8.11
C 2 (d)
7.84
C 7 and C 8 (m)
7.72
C 3 (d)
7.23
C 11 (s)
4.15
f1 (ppm)

(a)

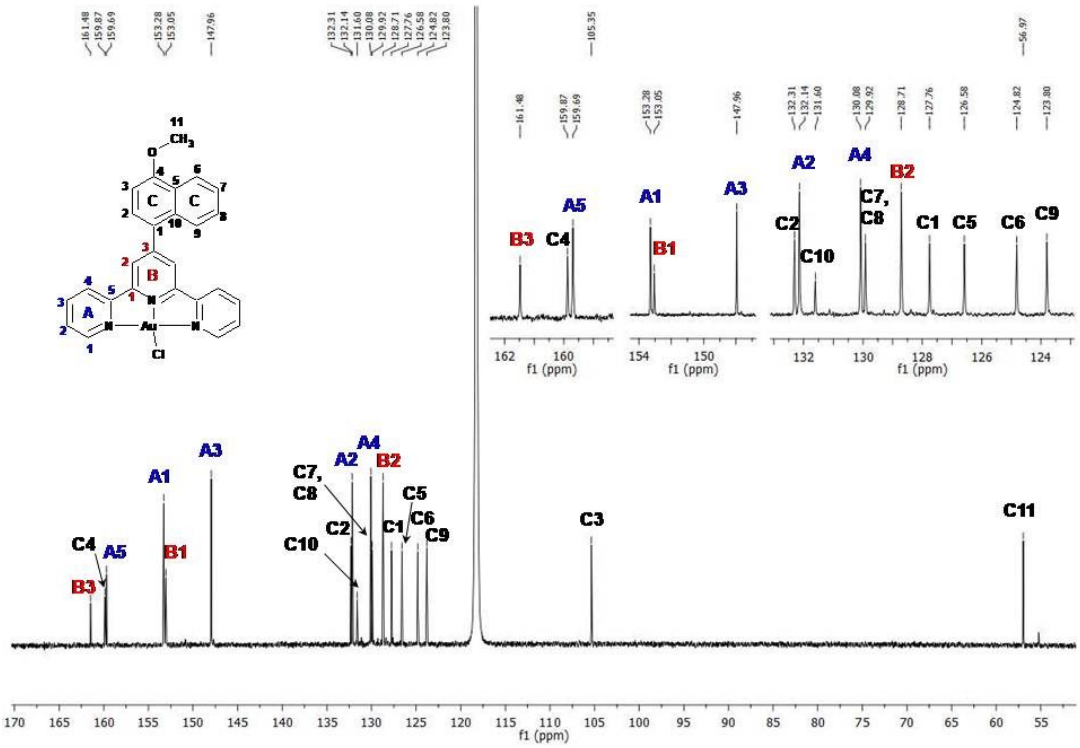
A1
A2
A3
A4
A5
B1
B2
B3
C1
C2
C3
C4
C5
C6
C7, C8
C9
C10
C11
f1 (ppm)

(b)

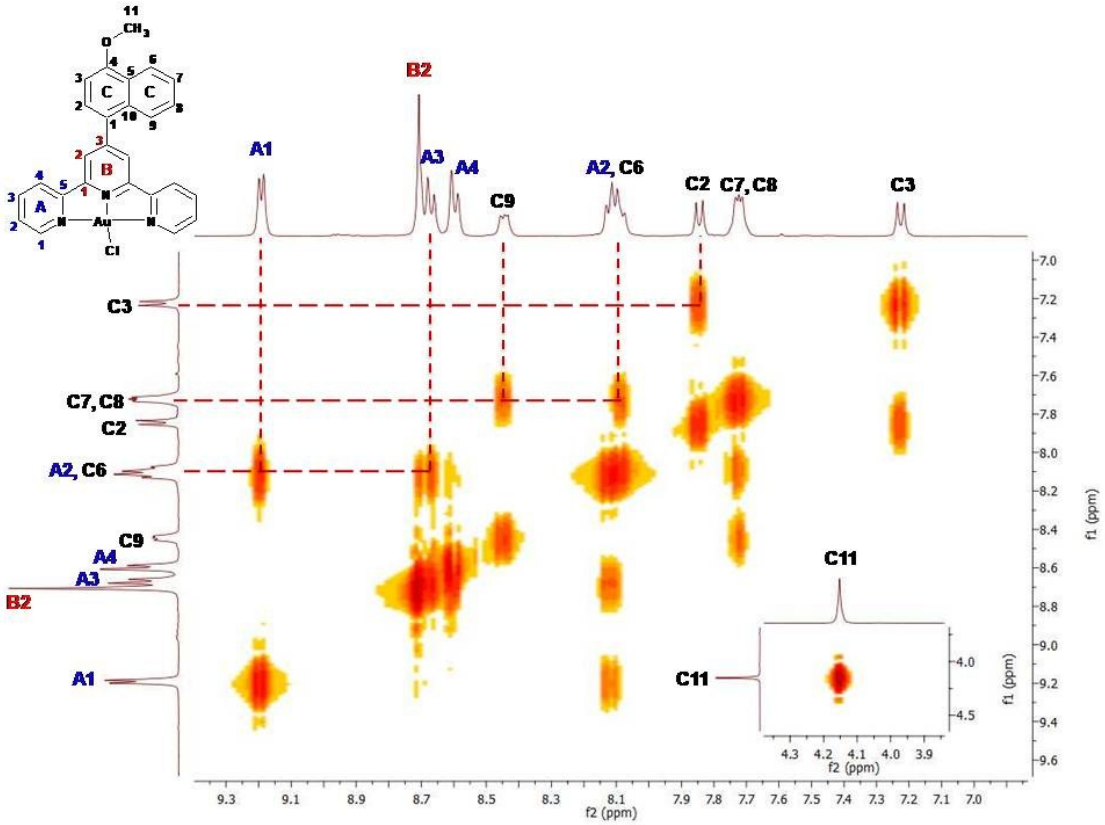
A1
B2
A3
A4
C9
A2, C6
C2
C7, C8
C3
C11
f2 (ppm)
f1 (ppm)

(c)

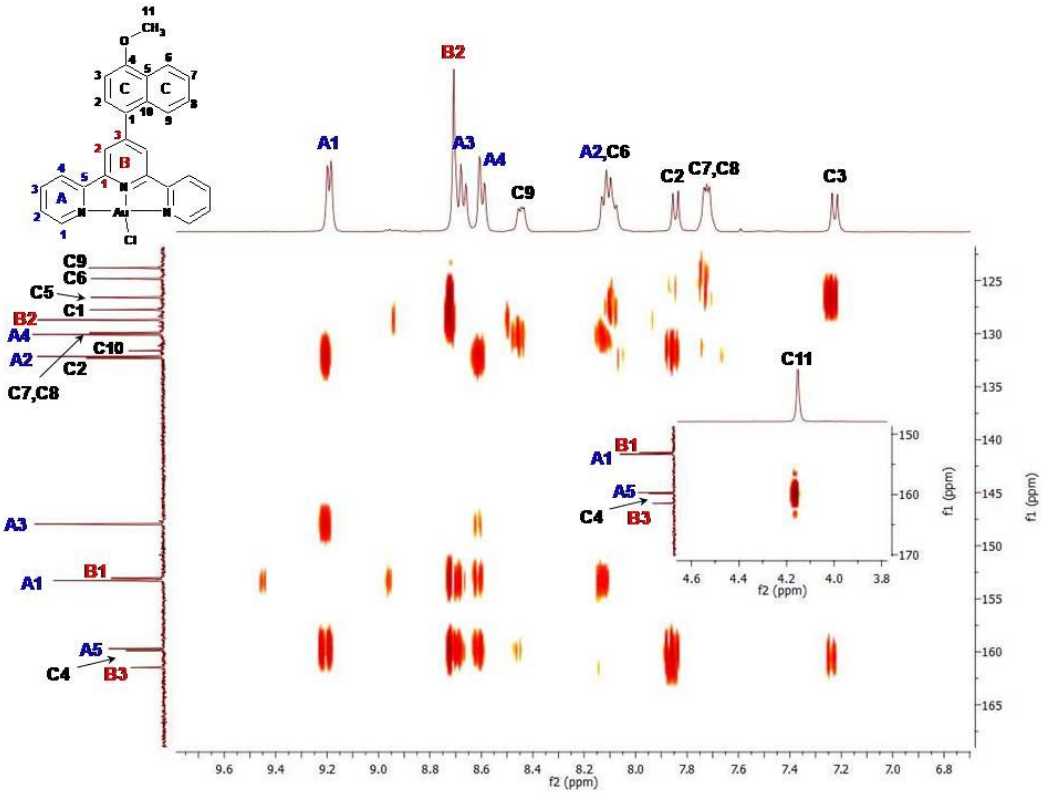
A1
B2
A3
A4
C9
A2,C6
C2
C7,C8
C3
C11
B1
A5
C4
B3
f2 (ppm)
f1 (ppm)

(d)

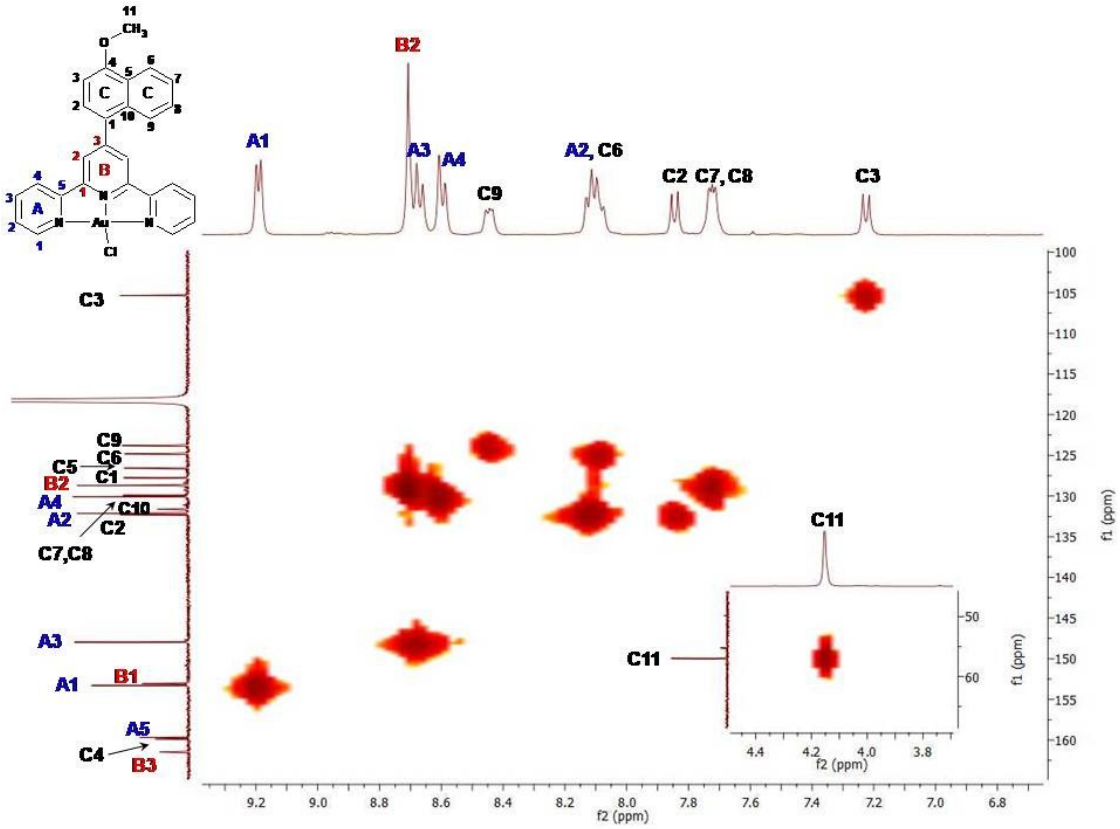

(e)

Figure S3. ^{1}H NMR (a), ^{13}C NMR (b), COSY (c), HMBC (d) and HMQC (e) NMR of **2.**

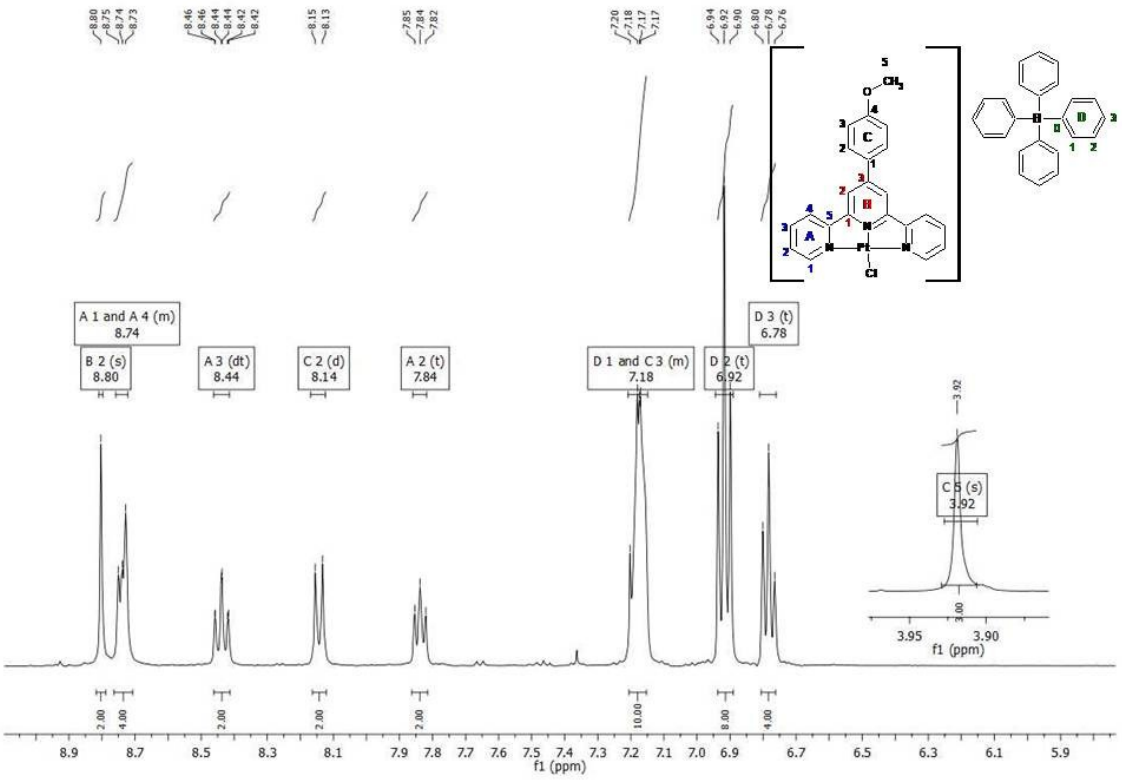
A 1 and A 4 (m)
8.74
B 2 (s)
8.80
A 3 (dt)
8.44
C 2 (d)
8.14
A 2 (t)
7.84
D 1 and C 3 (m)
7.18
D 2 (t)
6.92
D 3 (t)
6.78
C 5 (s)
3.92
f1 (ppm)

(a)

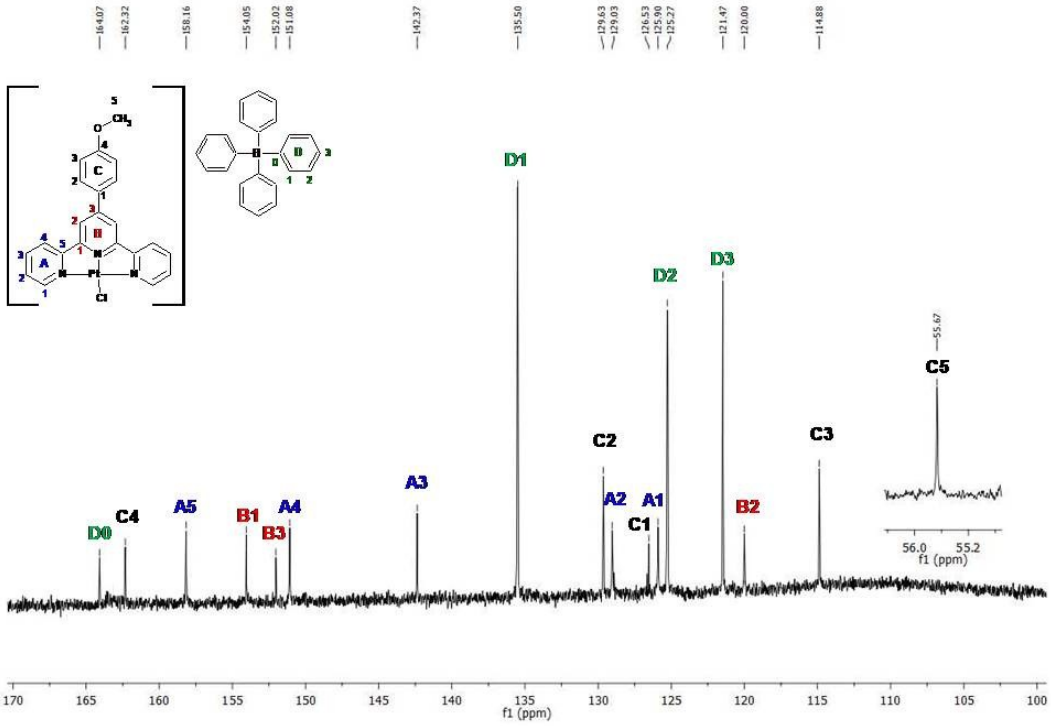
D0
C4
A5
B1
B3
A4
A3
D1
C2
A2
C1
A1
D2
D3
B2
C3
C5
f1 (ppm)

(b)

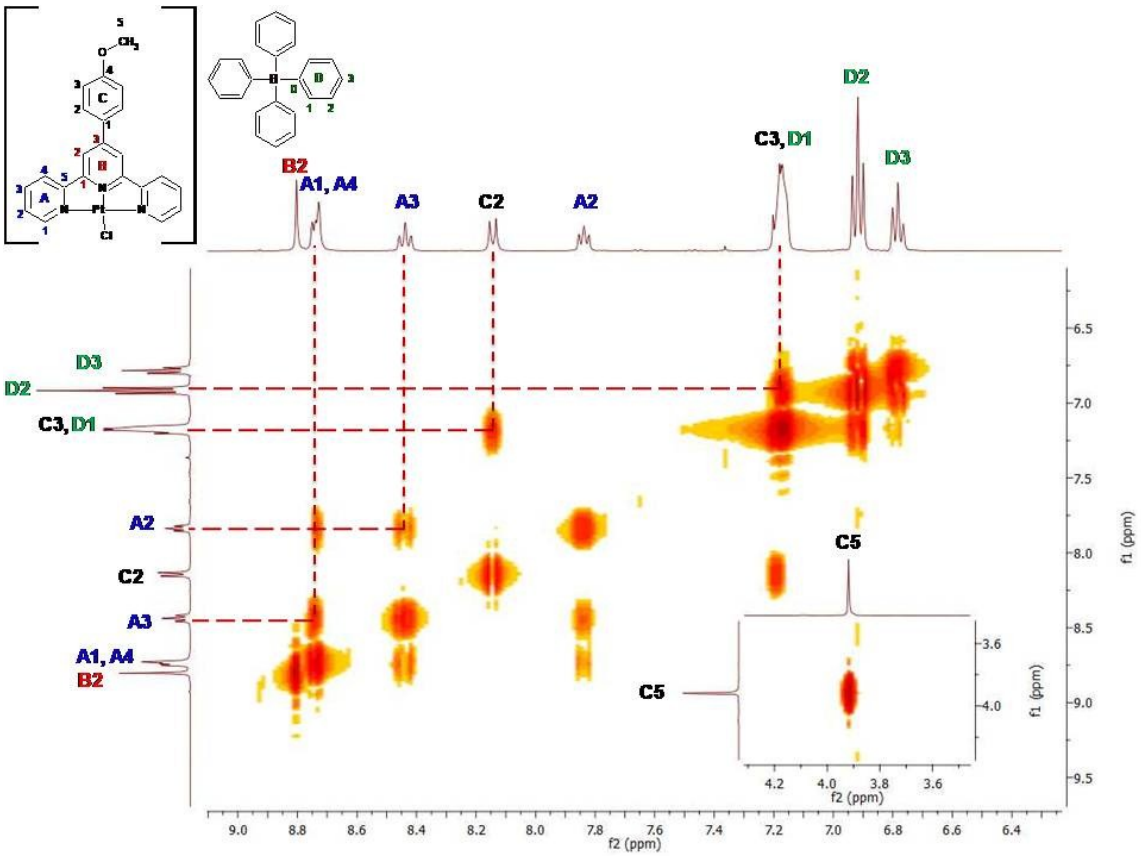
B2
A1, A4
A3
C2
A2
C3, D1
D2
D3
C5
f2 (ppm)
f1 (ppm)

(c)

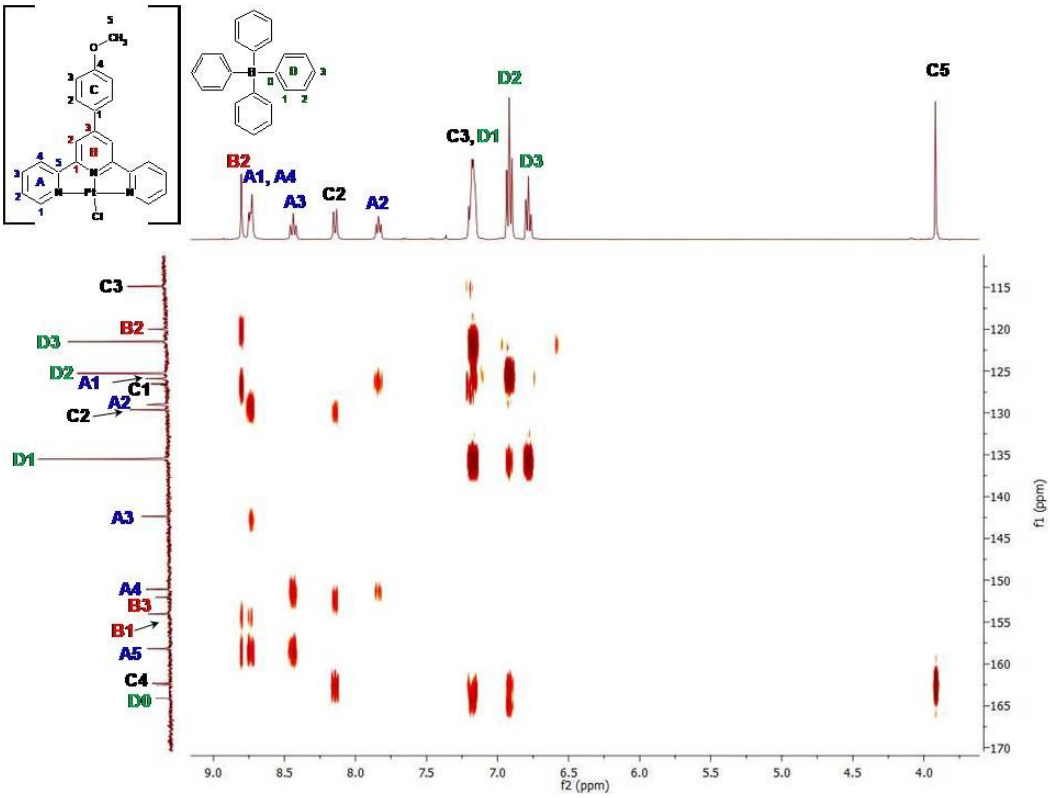
C5
D2
C3, D1
D3
B2
A1, A4
A3
C2
A2
C3
D1
A1
C1
A4
B3
B1
A5
C4
D0
f2 (ppm)
f1 (ppm)

(d)

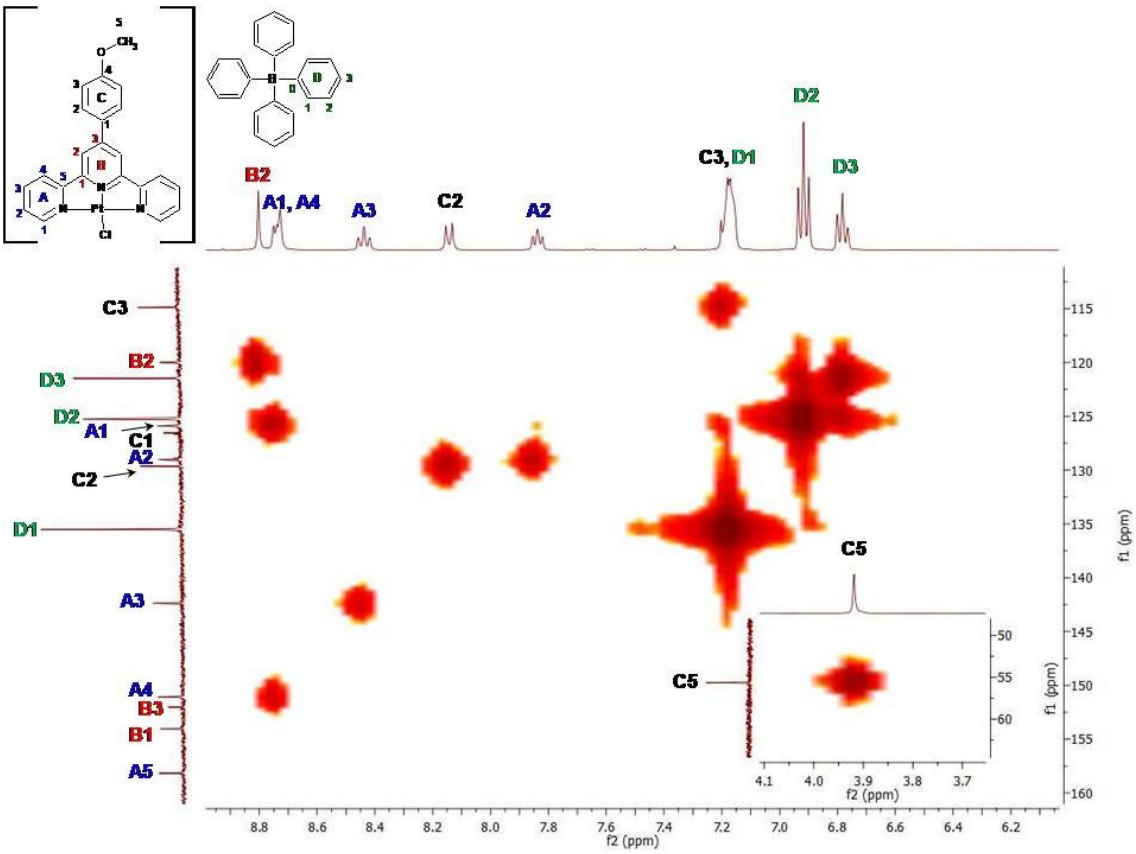

(e)

Figure S4. ^{1}H NMR (a), ^{13}C NMR (b), COSY (c), HMBC (d) and HMQC (e) NMR of **3**

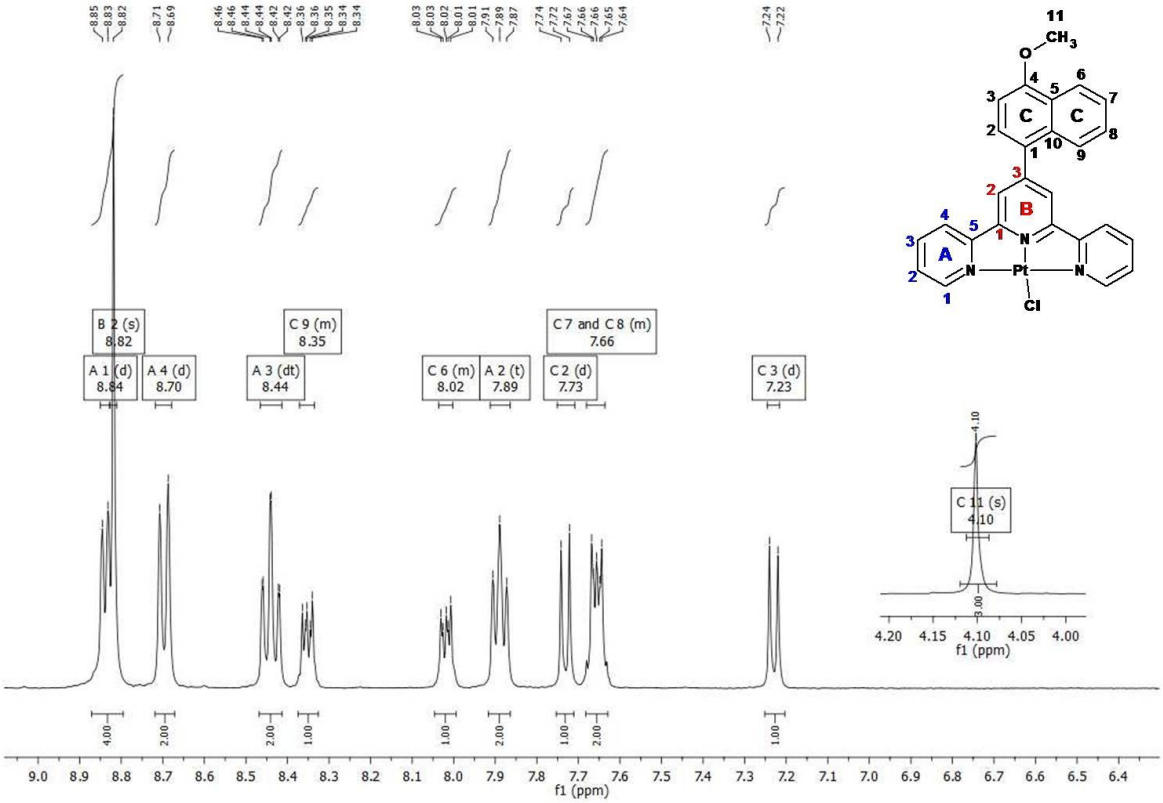
B 2 (s) 8.82
A 1 (d) 8.84
A 4 (d) 8.70
A 3 (dt) 8.44
C 9 (m) 8.35
C 6 (m) 8.02
A 2 (t) 7.89
C 2 (d) 7.73
C 7 and C 8 (m) 7.66
C 3 (d) 7.23
C 11 (s) 4.10
f1 (ppm)

(a)

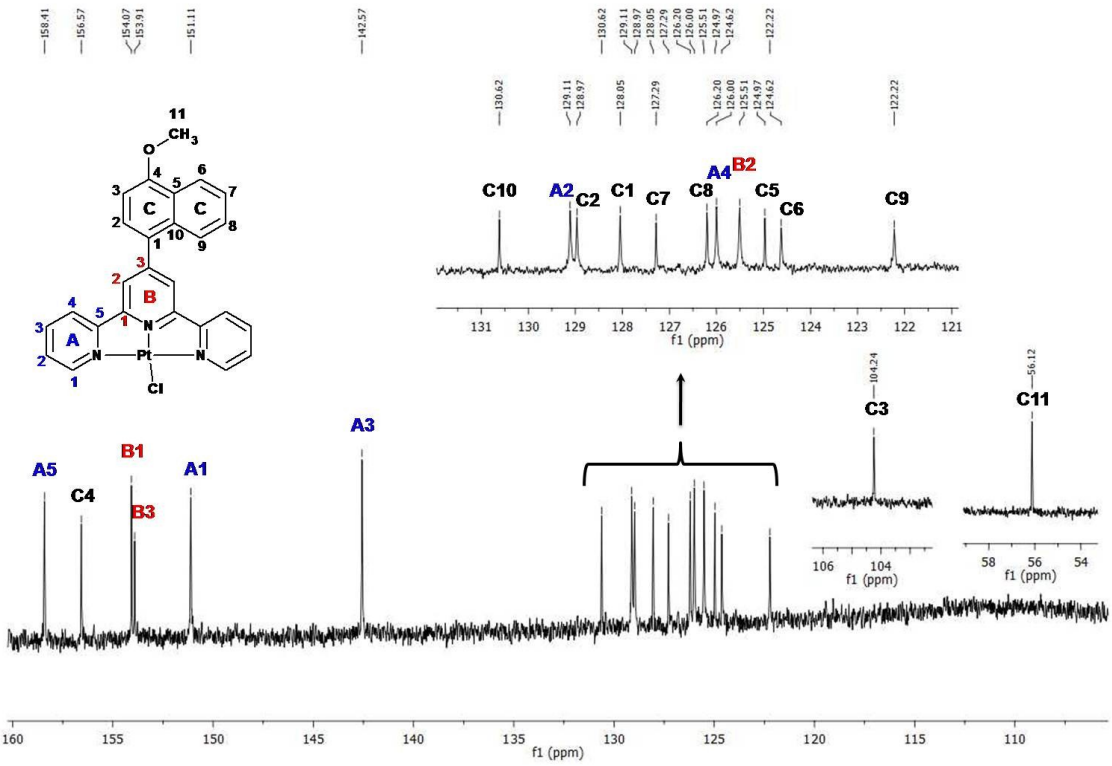
C10
A2
C2
C1
C7
C8
A4
B2
C5
C6
C9
A5
C4
B1
B3
A1
A3
C3
C11
f1 (ppm)

(b)

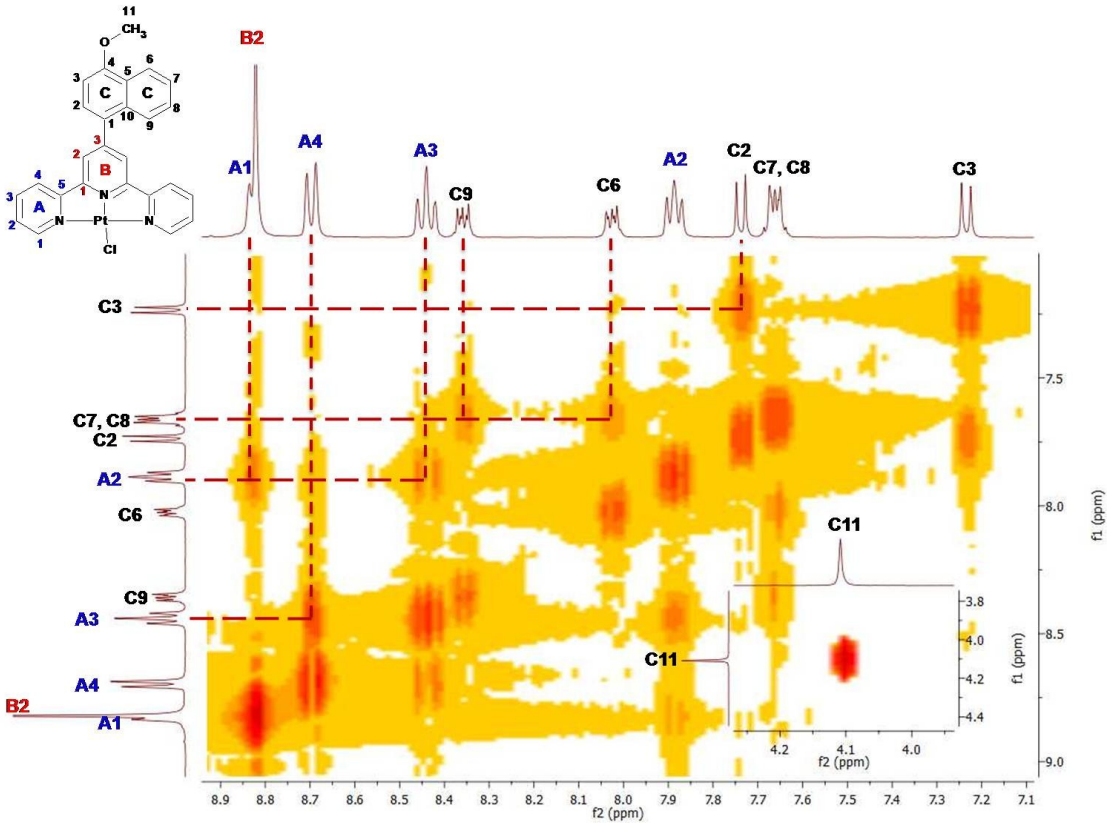
B2
A1
A4
A3
C9
C6
A2
C2
C7, C8
C3
C11
f2 (ppm)
f1 (ppm)

(c)

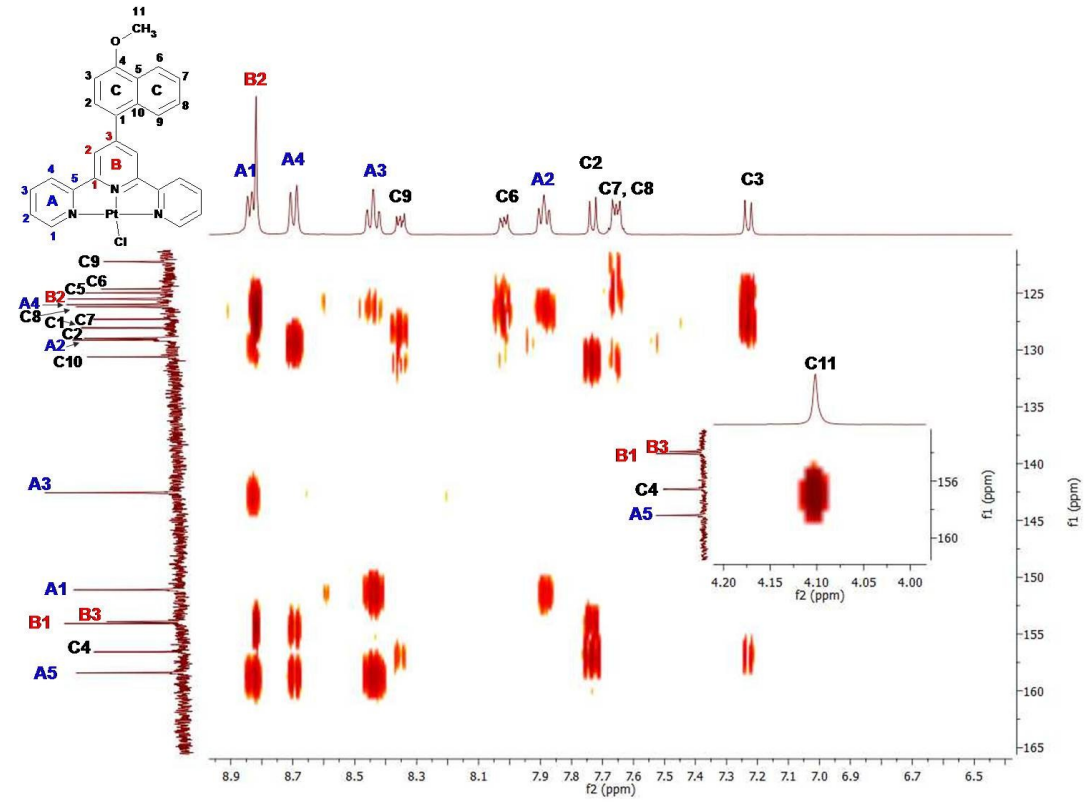
B2
A1
A4
A3
C9
C6
A2
C2
C7, C8
C3
C11
B1
B3
C4
A5
f2 (ppm)
f1 (ppm)

(d)

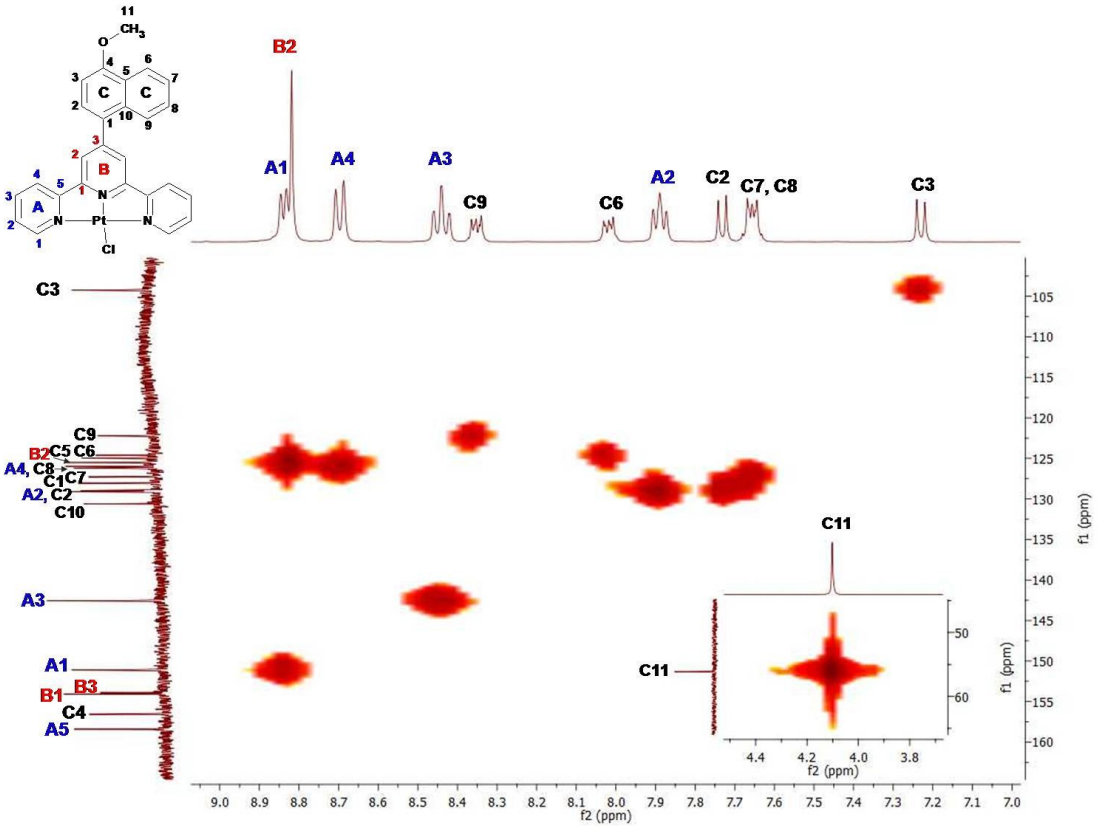

(e)

Figure S5. ^{1}H NMR (a), ^{13}C NMR (b), COSY (c), HMBC (d) and HMQC (e) NMR of **4**.

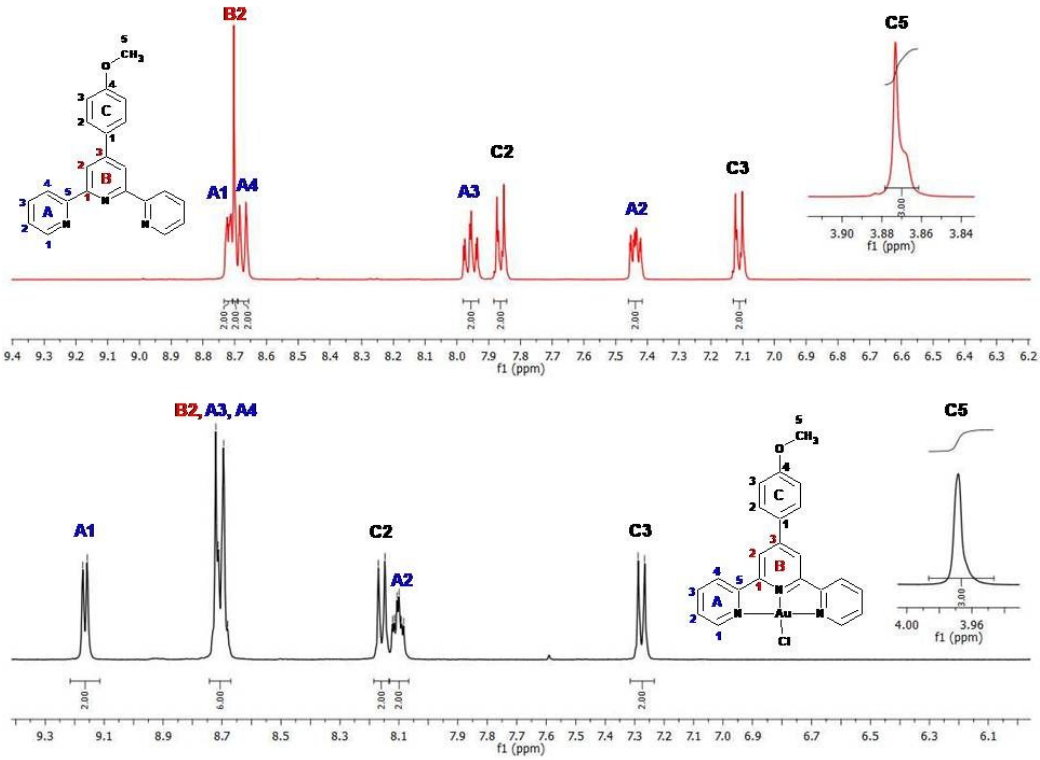

(a)

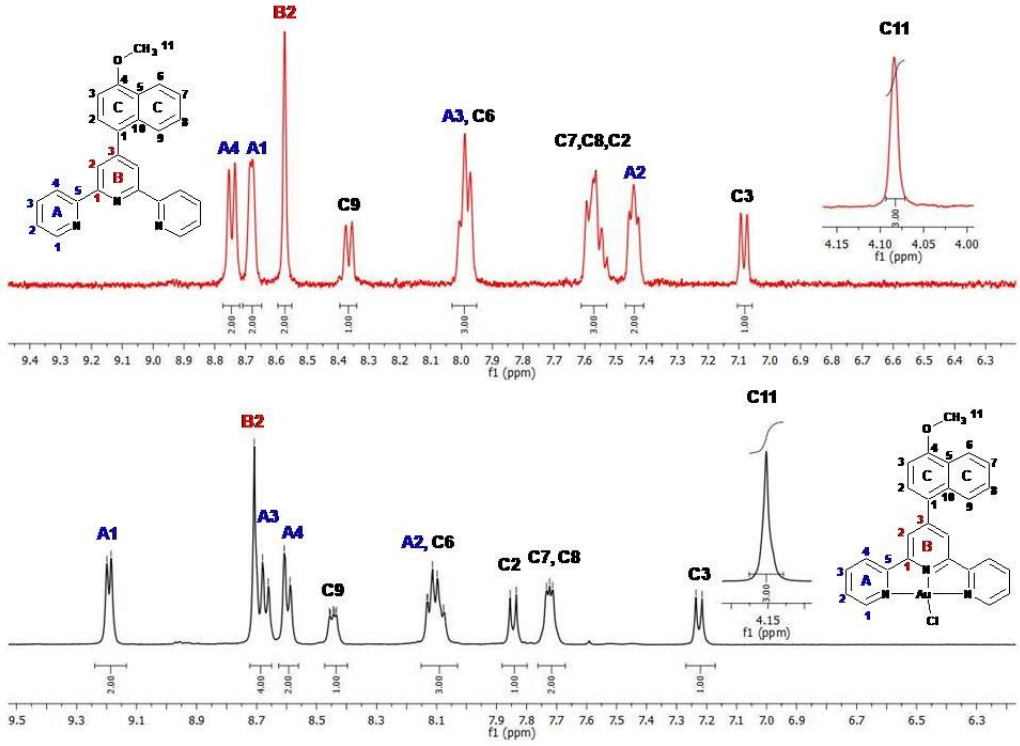

(b)

Figure S6. Comparison of ^{1}H NMR of **1** (a) or **2** (b) with the corresponding ligand L^1 and L^2 in acetonitrile-d_3.

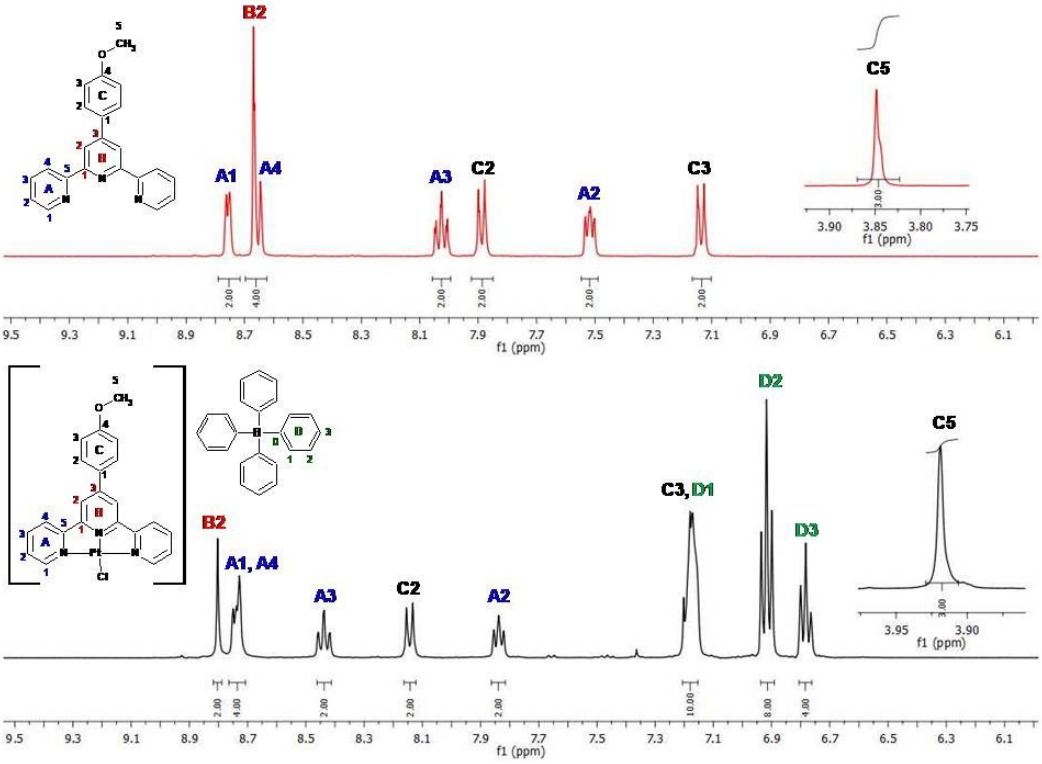

(a)

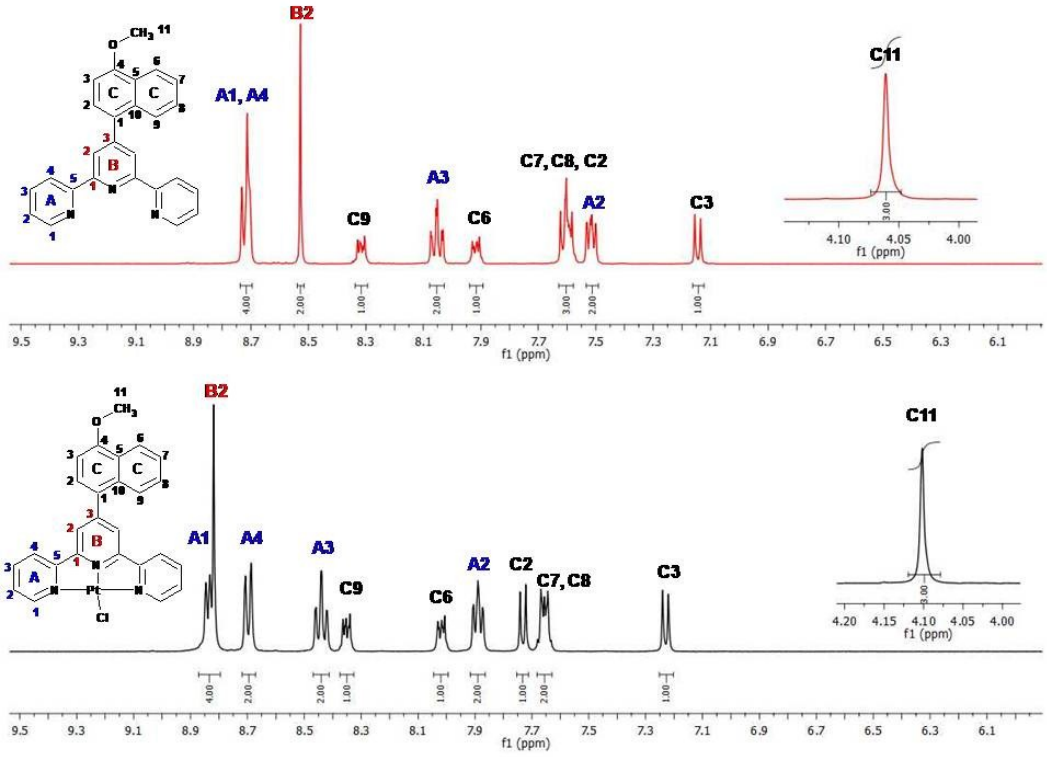

(b)

Figure S7. Comparison of ^{1}H NMR of **3** (a) or **4** (b) with the corresponding ligand L^1 and L^2 in DMSO-d_6.

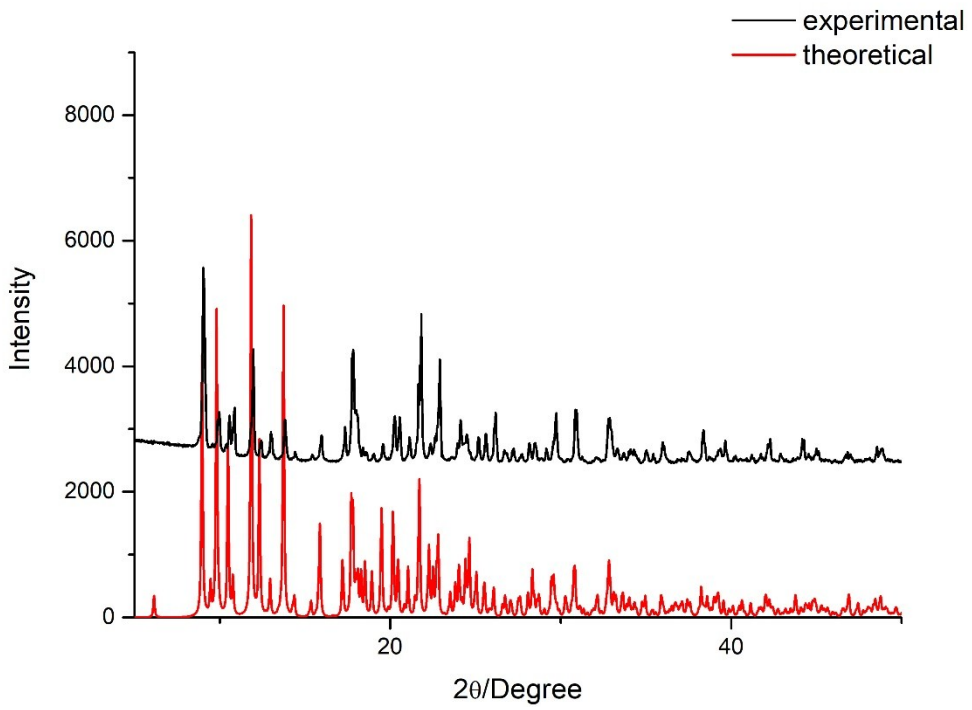

(a)

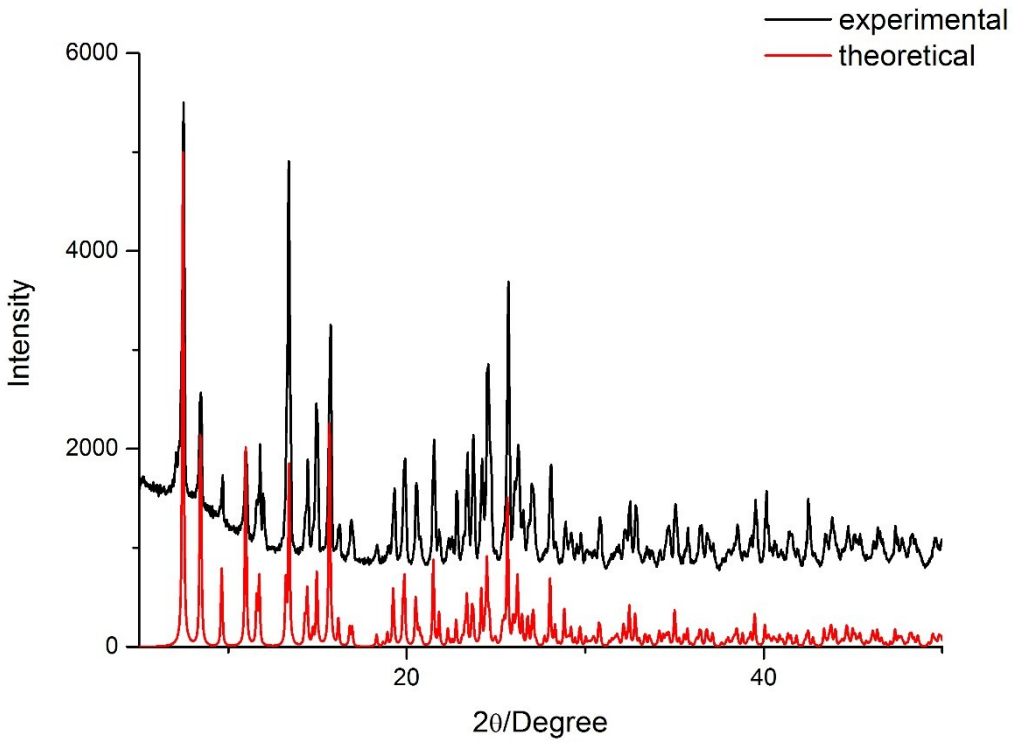

(b)

Figure S8. The powder XPRD patterns of representative compounds **1** (a) and **4** (b) (experimental - black) and the simulations of the powder pattern from the crystal structures (red).

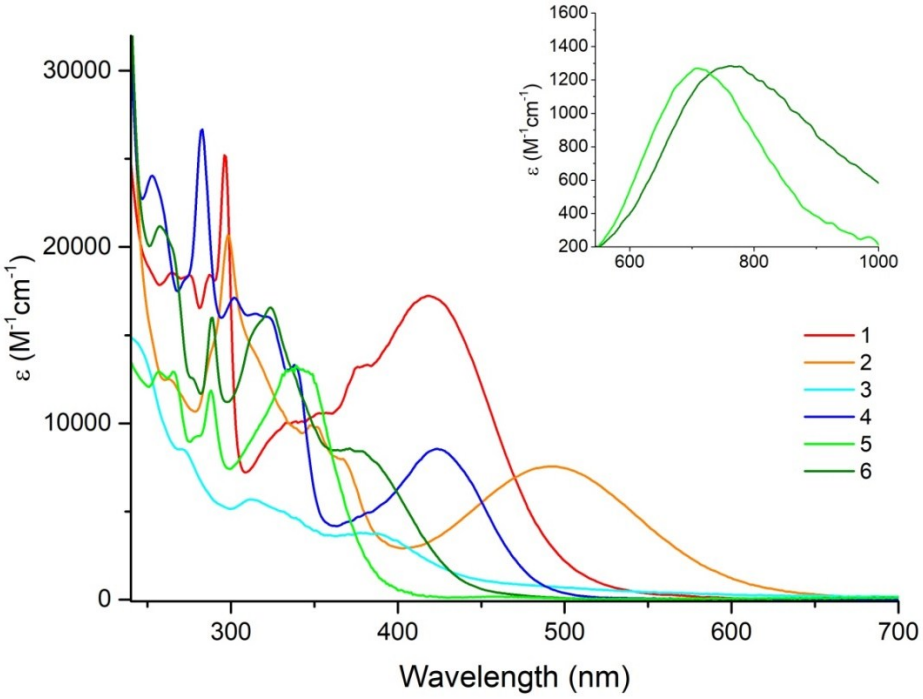

Figure S9. UV-Vis spectra of the complexes **1-6** in CH_3CN ($c = 5 \cdot 10^{-5}$ M)

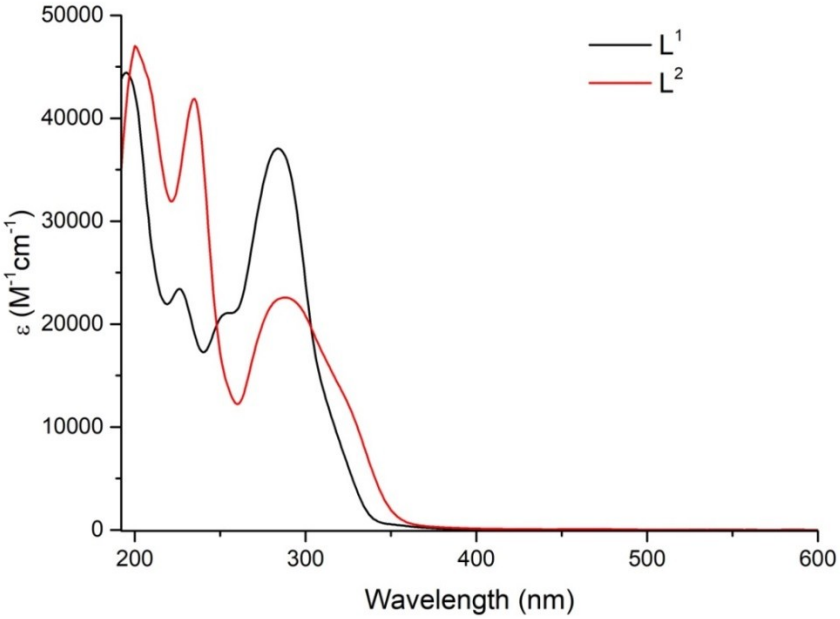

Figure S10. UV-vis spectra of the free ligands in CH_3CN ($5 \cdot 10^{-5}$ M).

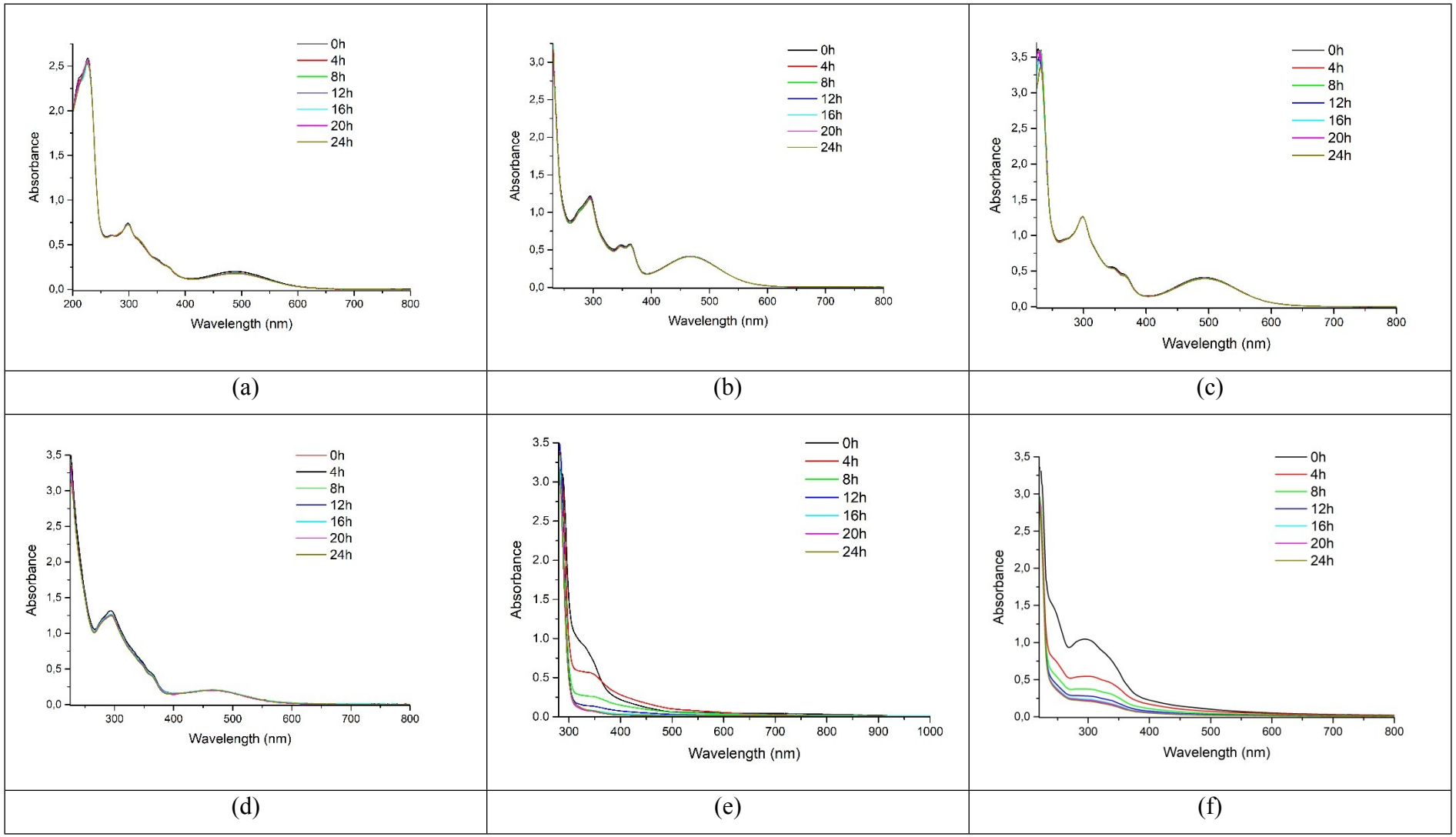

Figure S11. UV-Vis absorption spectra of **2** in CH_3CN ($5 \cdot 10^{-5}$ M) (a), PBS buffer (pH 7.4, 130 mM NaCl) (b), CH_3OH:CH_3CH_2OH (1:4 v/v) (c), PBS upon addition of stoichiometric amount of glutathione (d), PBS upon addition of excess of glutathione (e) and PBS in the presence of sodium ascorbate (f). Spectra were recorded once every four hours for 24 h.

medium	Excitation and emission spectra	PL lifetime curve
	1	
MeCN	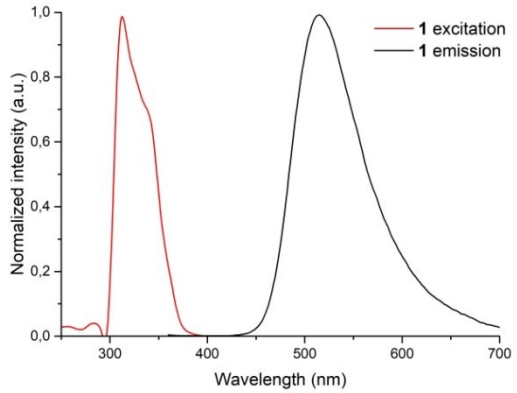	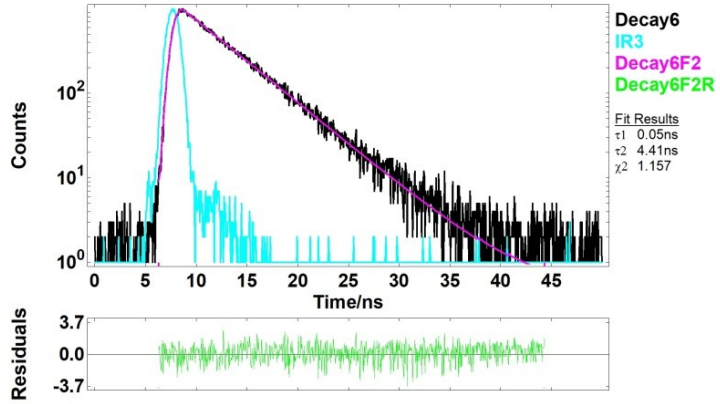
77K	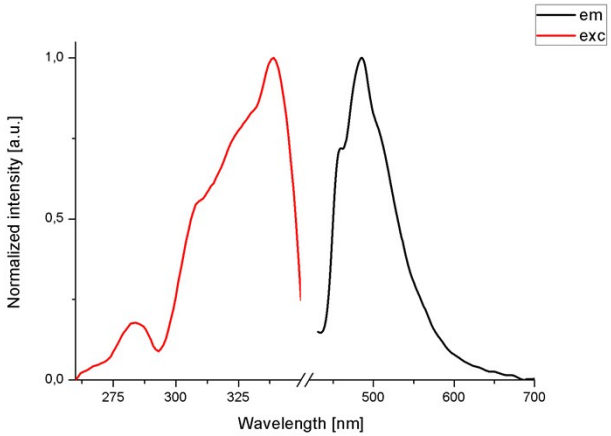	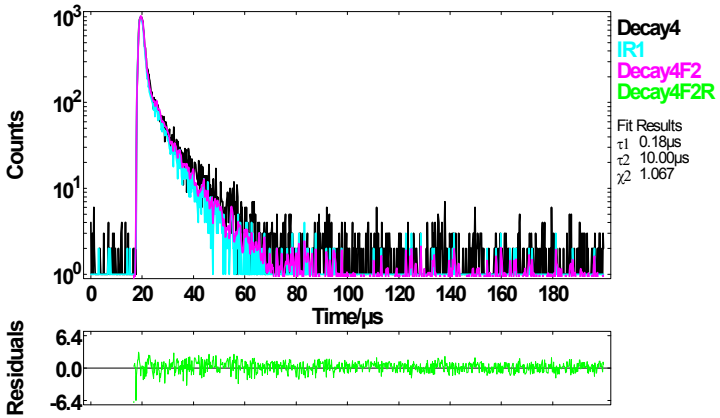

2		
MeCN	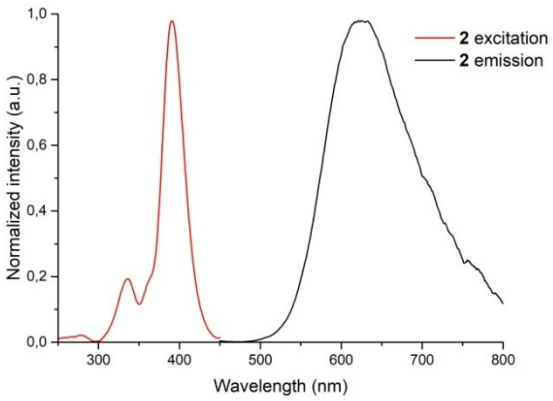 2 excitation 2 emission Normalized intensity (a.u.) Wavelength (nm)	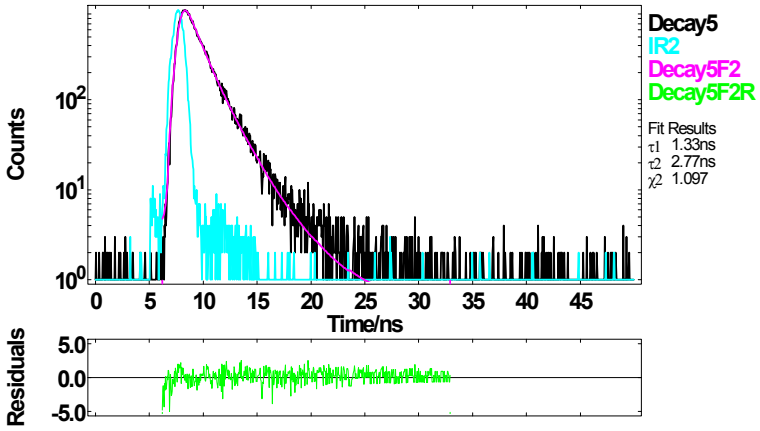 Decay5 IR2 Decay5F2 Decay5F2R Fit Results τ1 1.33ns τ2 2.77ns χ2 1.097 Counts Time/ns Residuals
77K	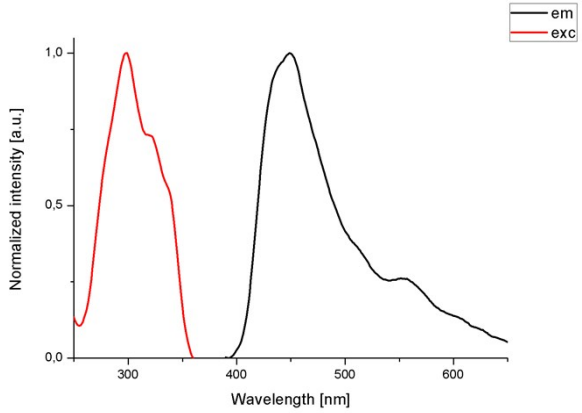 em exc Normalized intensity [a.u.] Wavelength [nm]	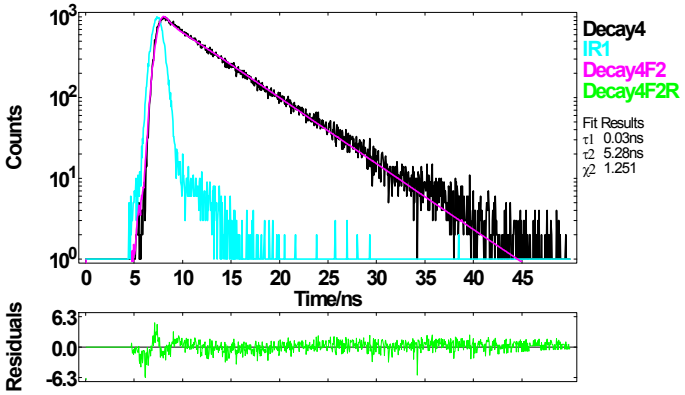 Decay4 IR1 Decay4F2 Decay4F2R Fit Results τ1 0.03ns τ2 5.28ns χ2 1.251 Counts Time/ns Residuals

3		
MeCN	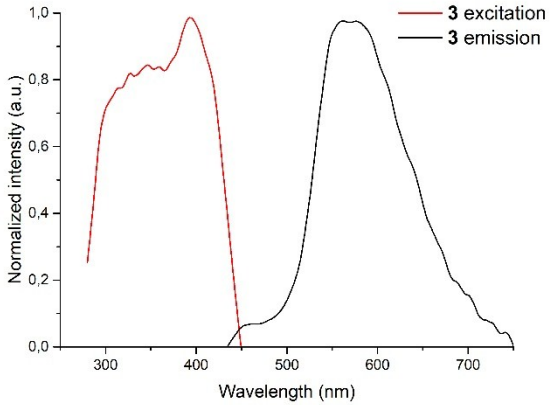 3 excitation 3 emission Normalized intensity (a.u.) Wavelength (nm)	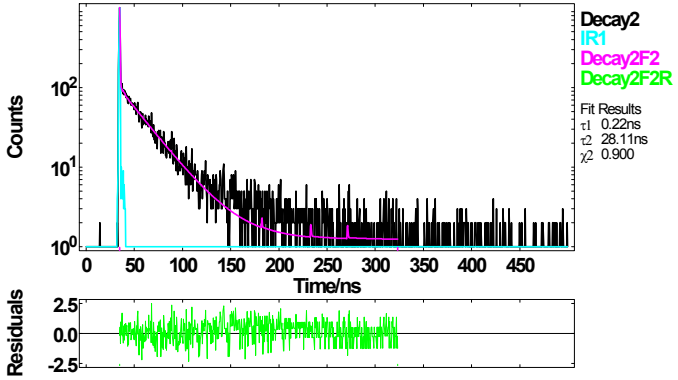 Decay2 IR1 Decay2F2 Decay2F2R Fit Results τ1 0.22ns τ2 28.11ns χ2 0.900 Counts Time/ns Residuals
77K	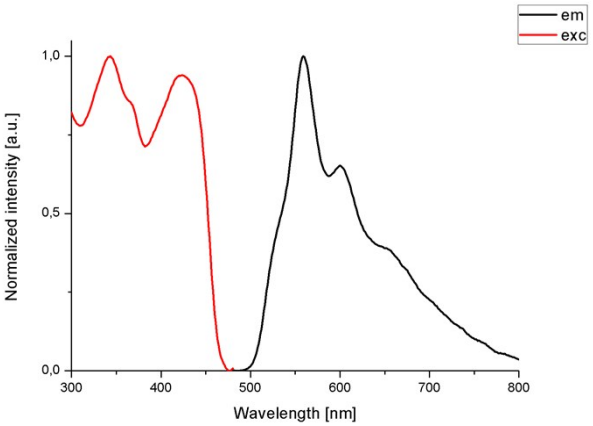 em exc Normalized intensity [a.u.] Wavelength [nm]	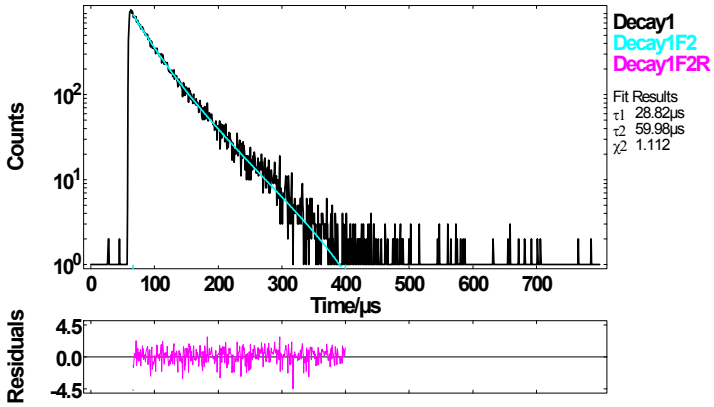 Decay1 Decay1F2 Decay1F2R Fit Results τ1 28.82µs τ2 59.98µs χ2 1.112 Counts Time/µs Residuals

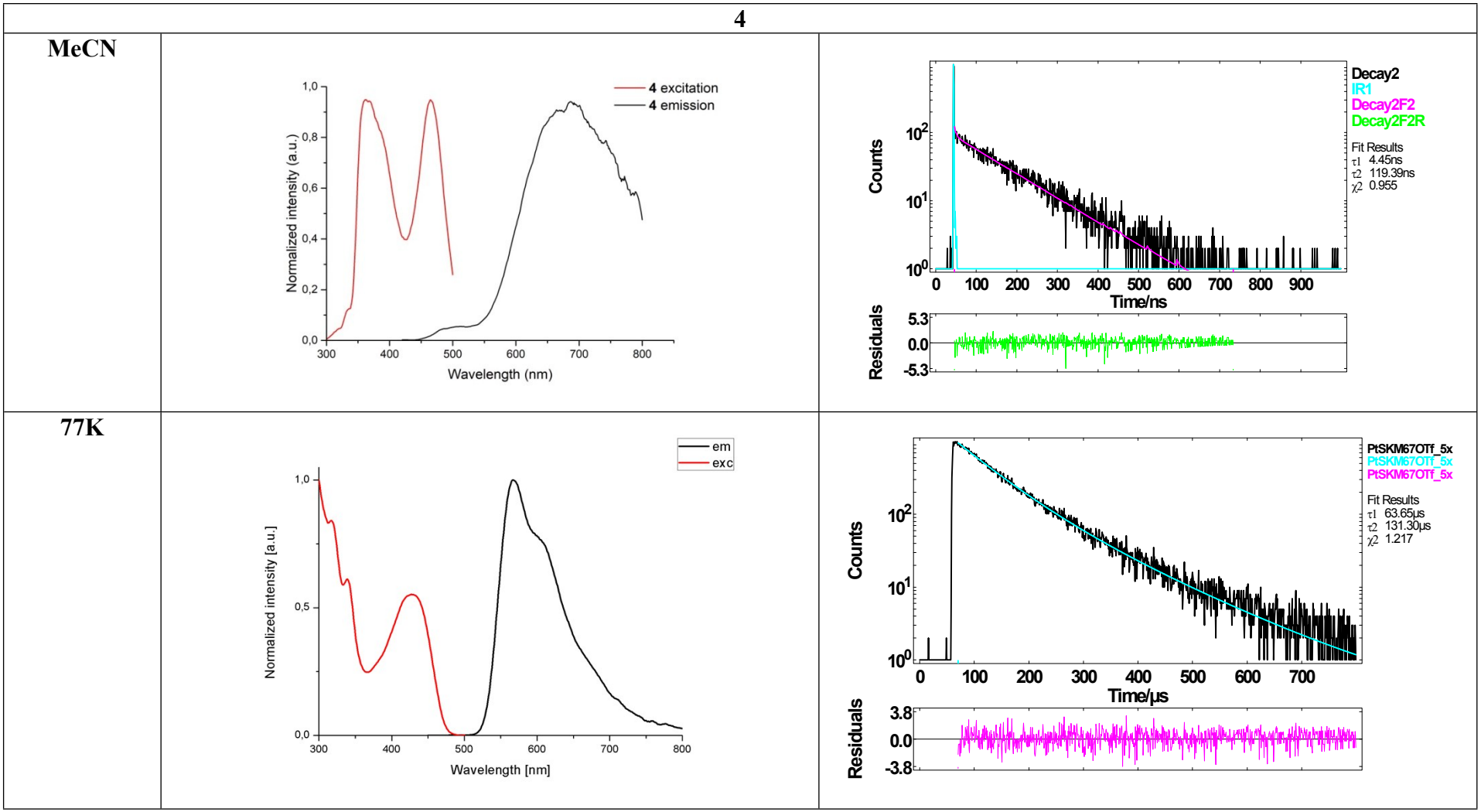

Figure S12. Excitation and emission spectra of compounds **1-4**.

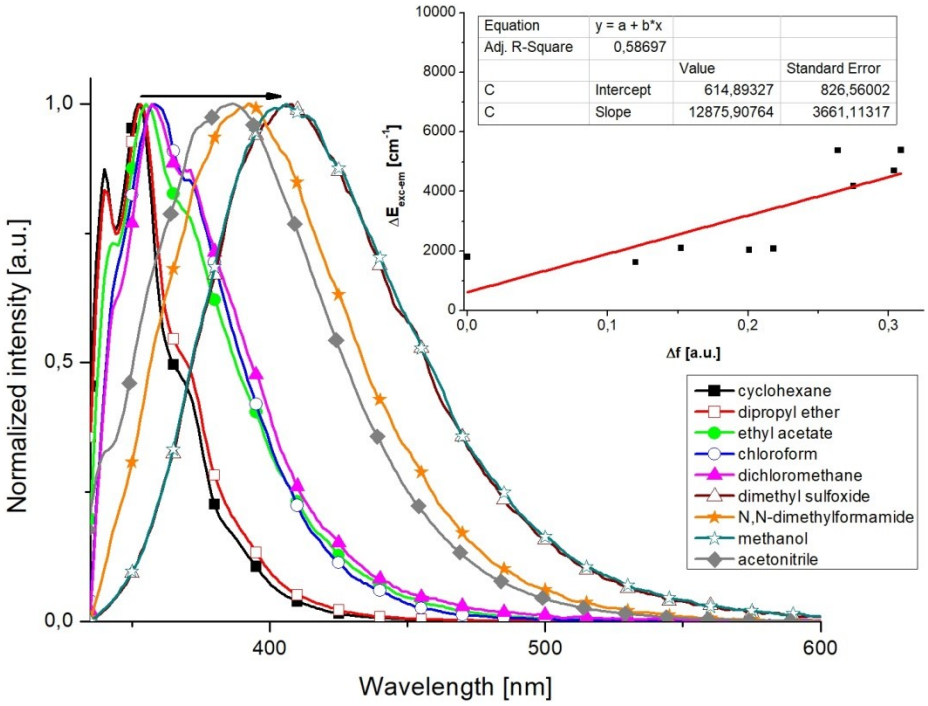

(a)

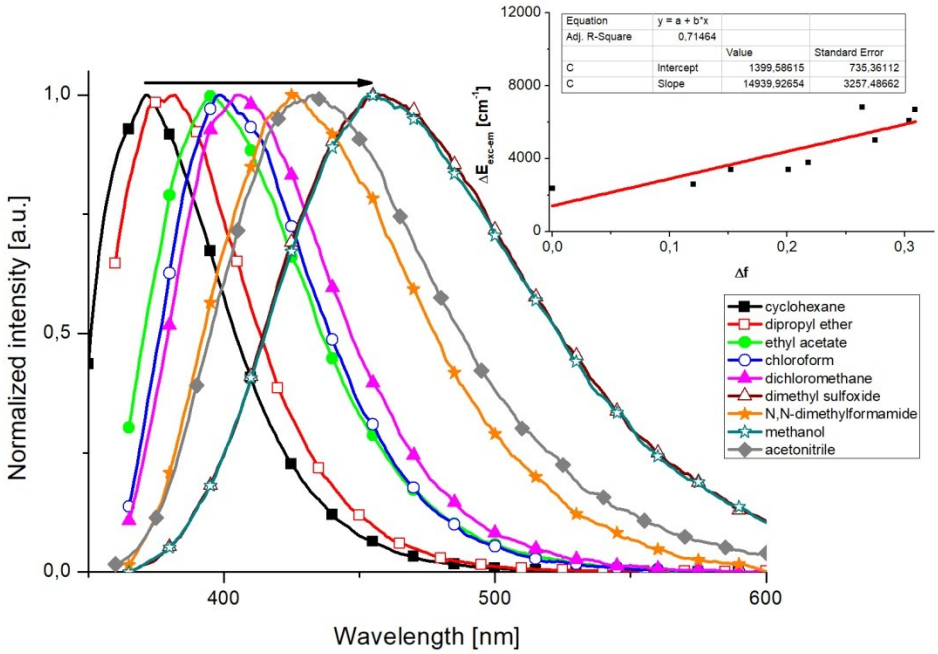

(b)

Figure S13. Emission spectra of **L**[1](a) and **L**[2] (b) in different solvents. Insert: Plot of Stokes shift $\Delta E_{exc\text{-}em}$ vs. solvent polarity parameter Δf

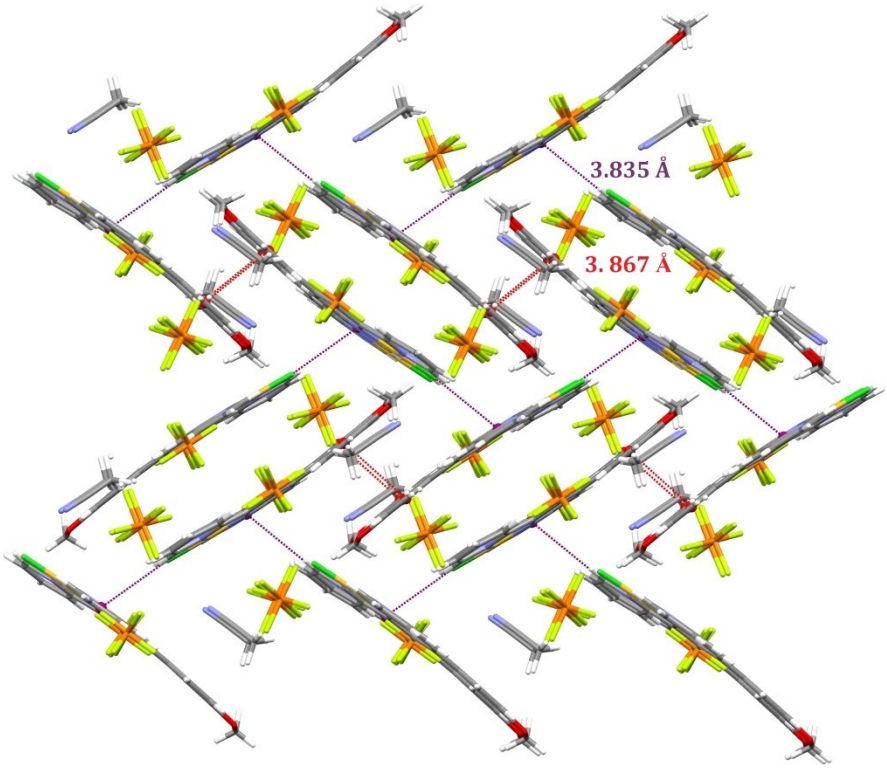

Figure S14. View of the supramolecular packing of **1** arising from weak π•••π and π•••Cl type interactions.

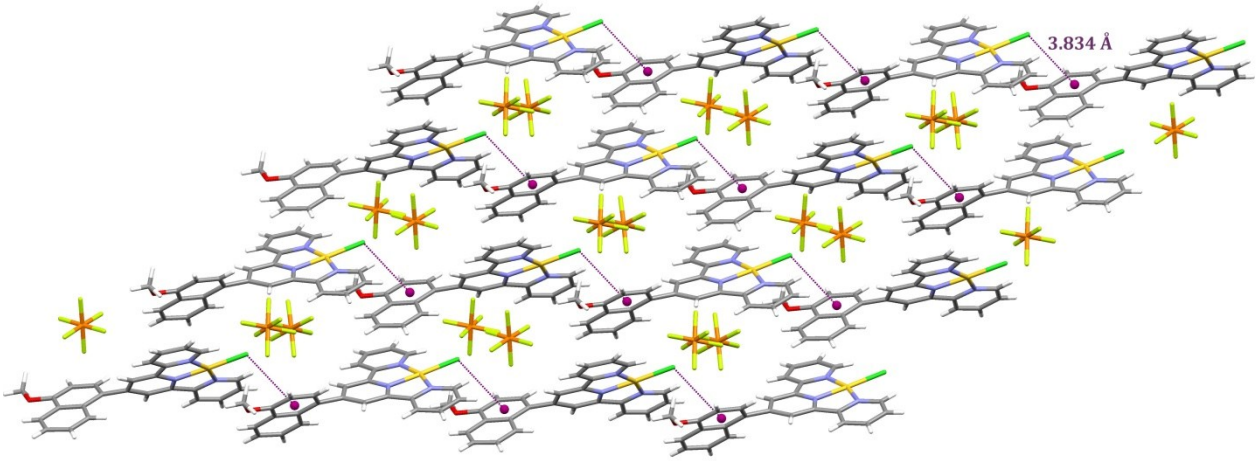

Figure S15. View of the supramolecular packing of **2** arising from weak π•••π and π•••Cl type interactions.

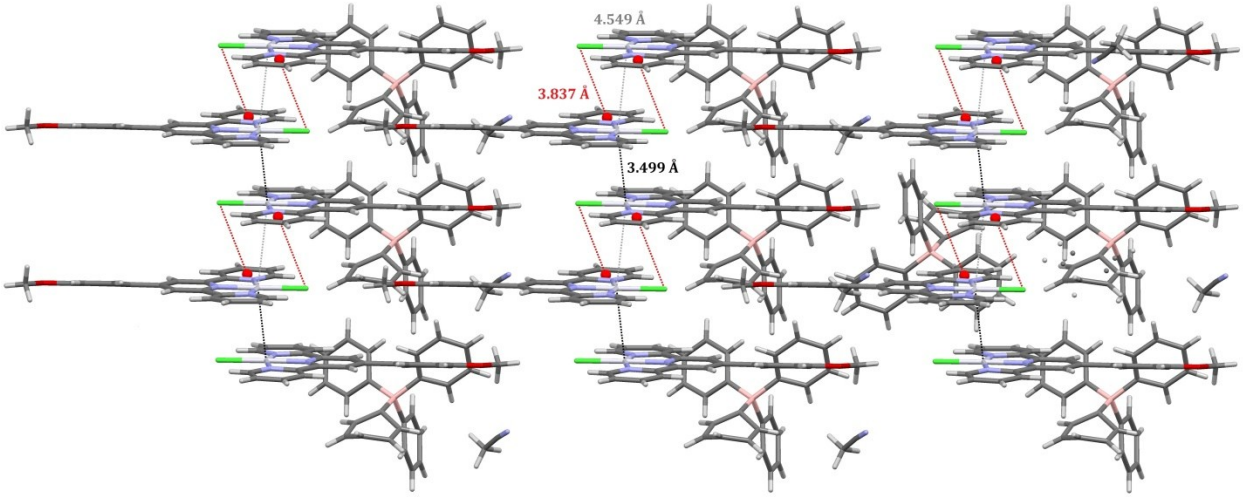

Figure S16. View of the supramolecular packing of **3** showing Cl···π (red dotted lines) interactions between $[PtCl(L^1)]^+$ cations and formation of a linear chain motifs with altering Pt···Pt distances of 3.499 and 4.549 Å.

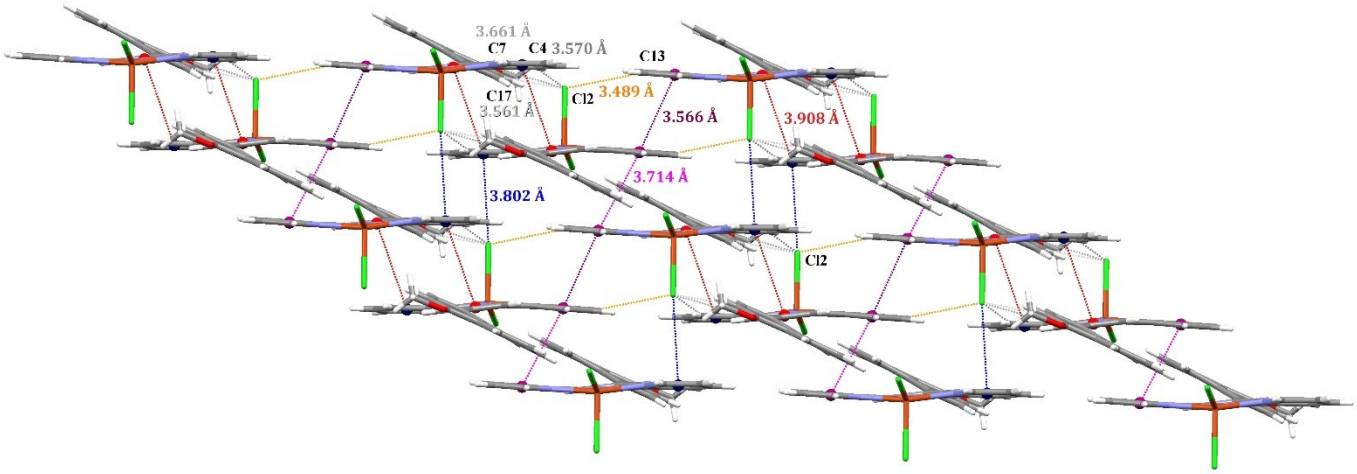

Figure S17. View of the supramolecular packing of the cations $[CuCl_2(L^2)]$ in **6**.

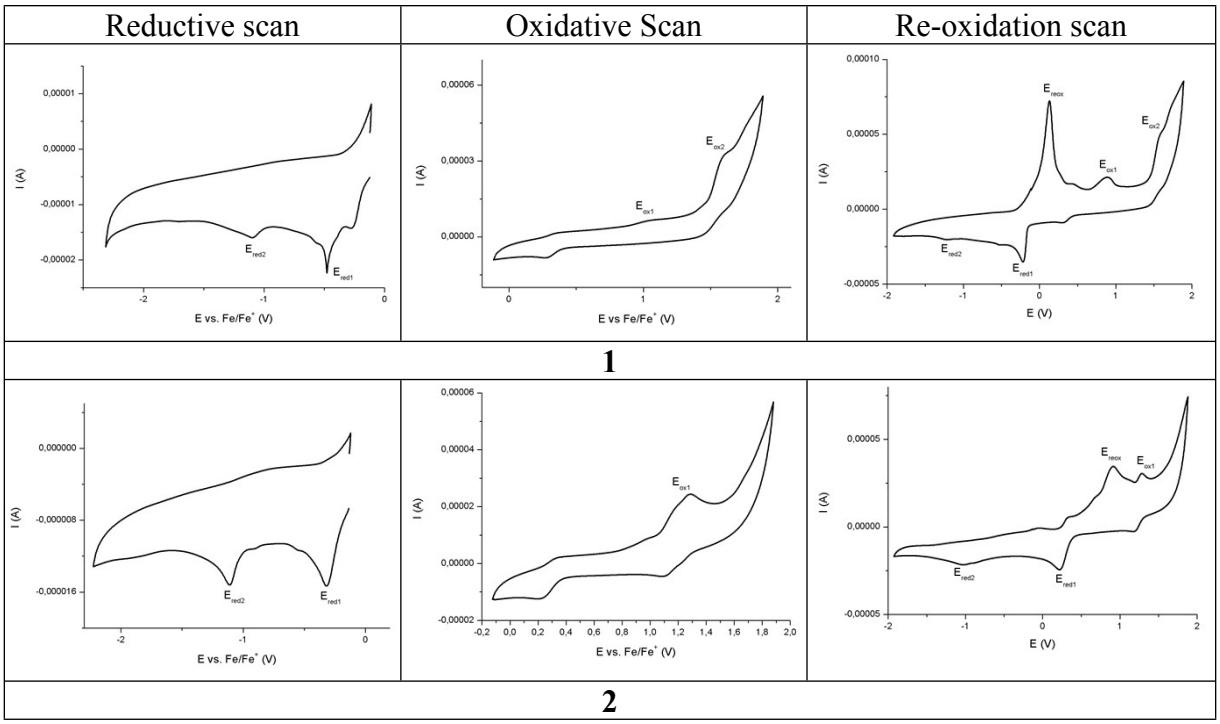

Figure S18. Cyclic voltammograms of compounds **1**–**2**.

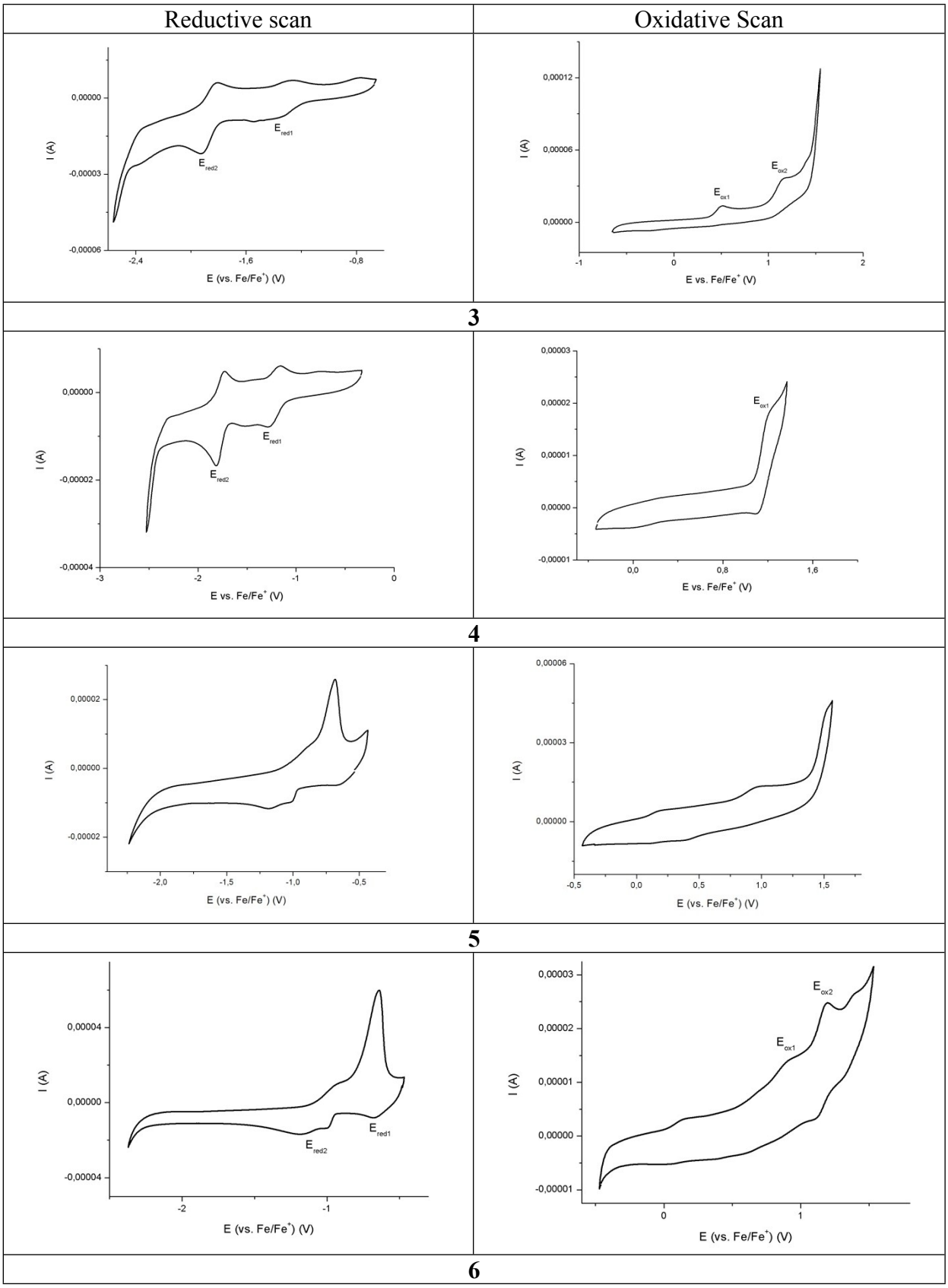

Figure S19. Cyclic voltammograms of compounds **3–6**.

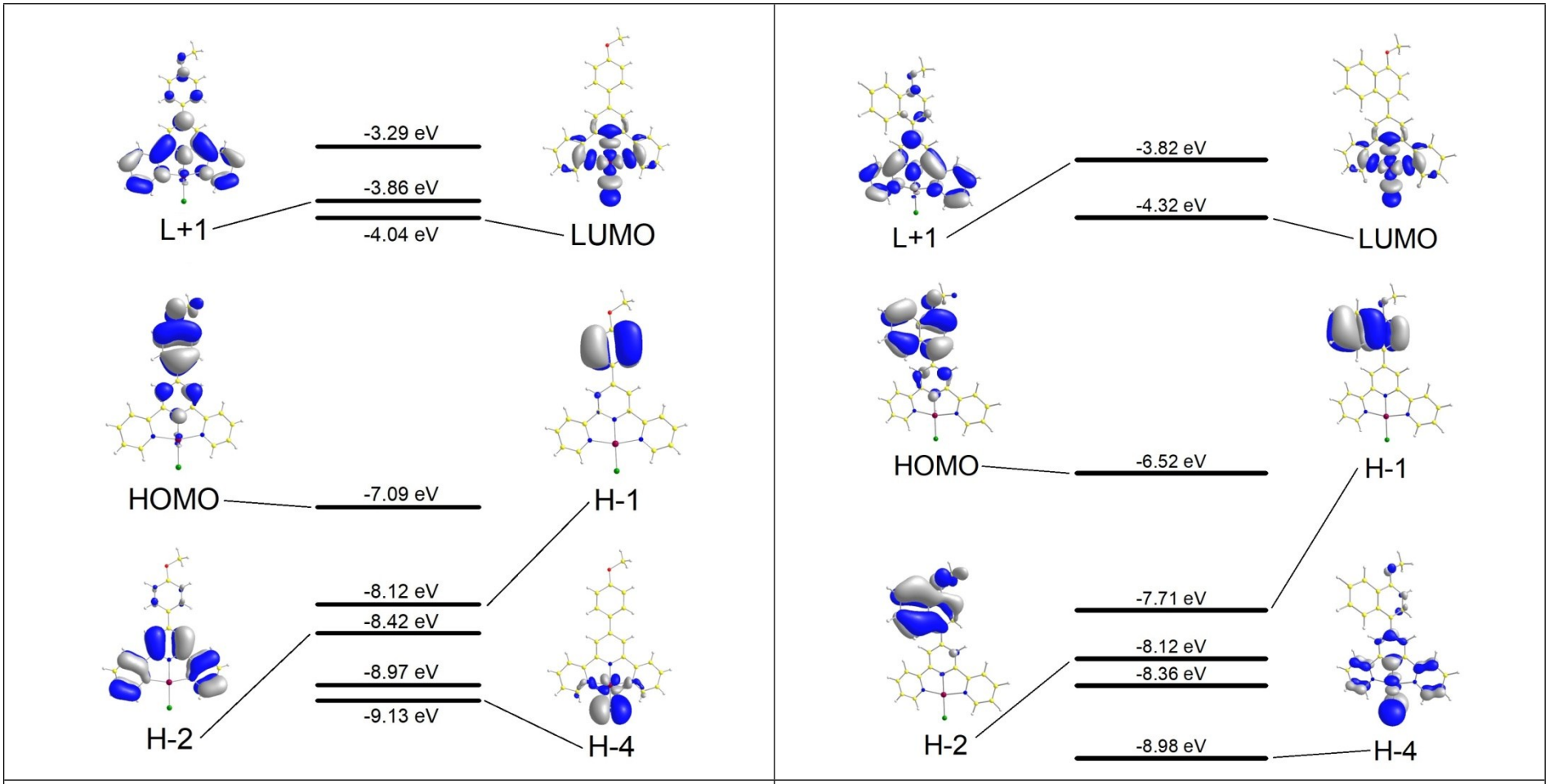
-3.29 eV
-3.86 eV
-4.04 eV
L+1
LUMO
HOMO
-7.09 eV
H-1
-8.12 eV
-8.42 eV
-8.97 eV
-9.13 eV
H-2
H-4
-3.82 eV
-4.32 eV
L+1
LUMO
HOMO
-6.52 eV
H-1
-7.71 eV
-8.12 eV
-8.36 eV
-8.98 eV
H-2
H-4

(a) (b)

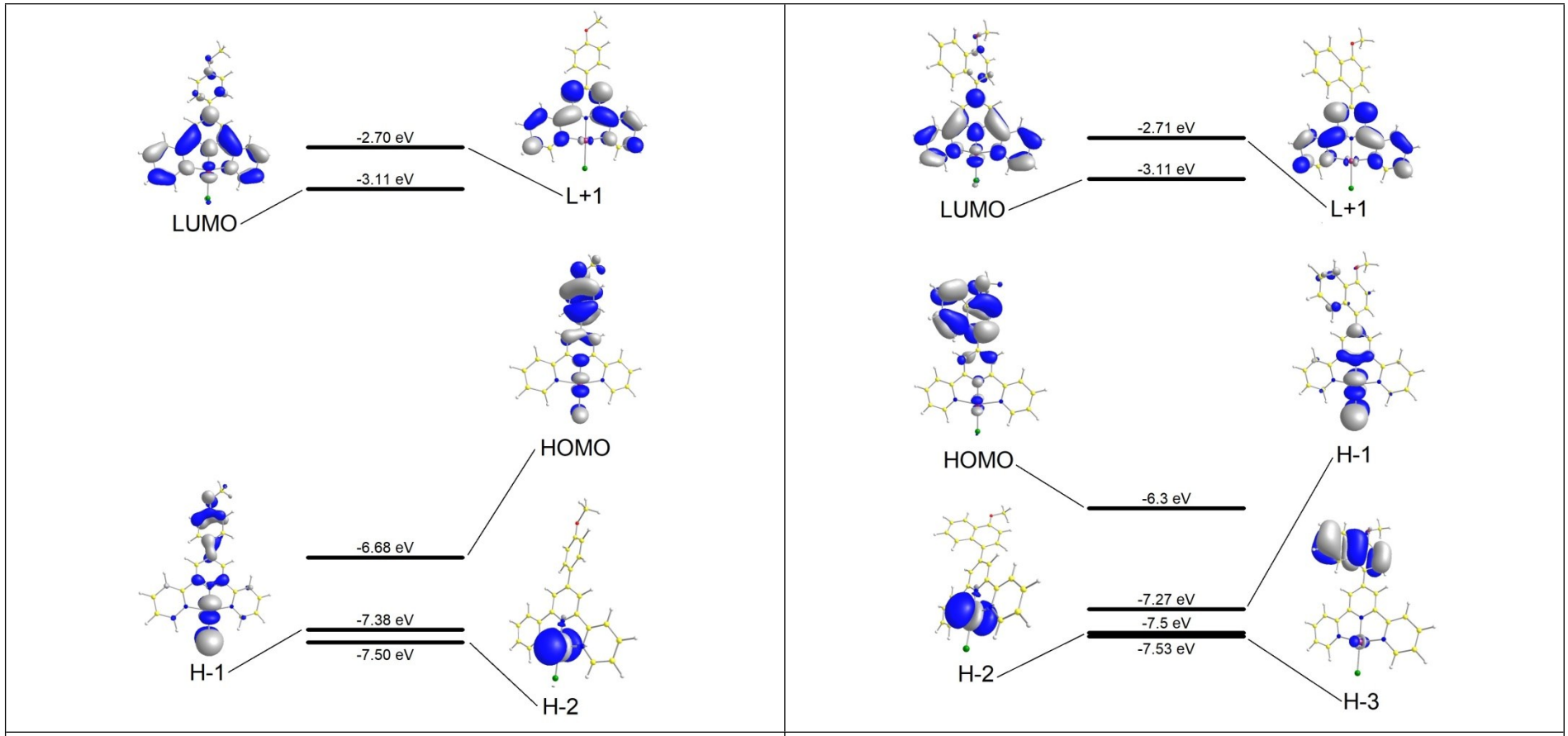

(c) (d)

Figure S20. Graphical representations of the selected MOs and their TD-DFT energies for **1-4** (a-d).

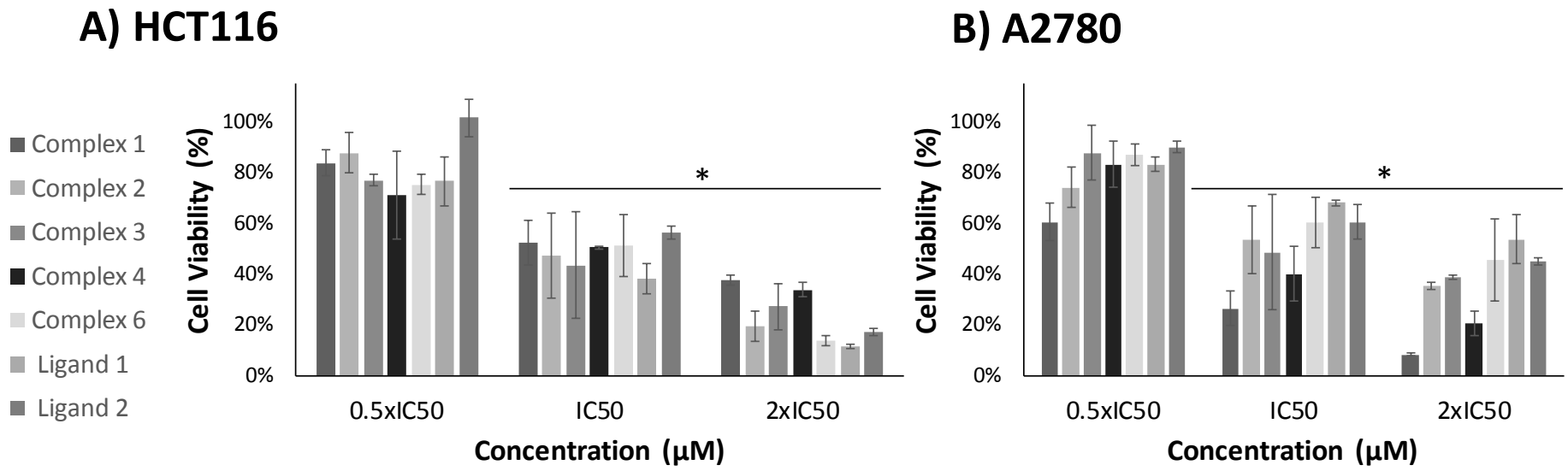

Figure S21. Cytotoxicity of metallic complexes **1-4**, **6** and ligands L^1 and L^2 in HCT116 (a) and A2780 (b) cell lines. Cells were incubated with $0.5xIC_{50}$, IC_{50} and $2xIC_{50}$ concentrations of complexes for 48 h and cell viability percentage was determined by the trypan blue exclusion method, using cells incubated with 0.1% (v/v) DMSO as control. The results shown are expressed as the mean ± SD from three independent assays. The symbol * means that the results are statistically significant with a $p < 0.05$ (as compared to $0.5xIC_{50}$ cell viability for compound concentration in the respective cell line).

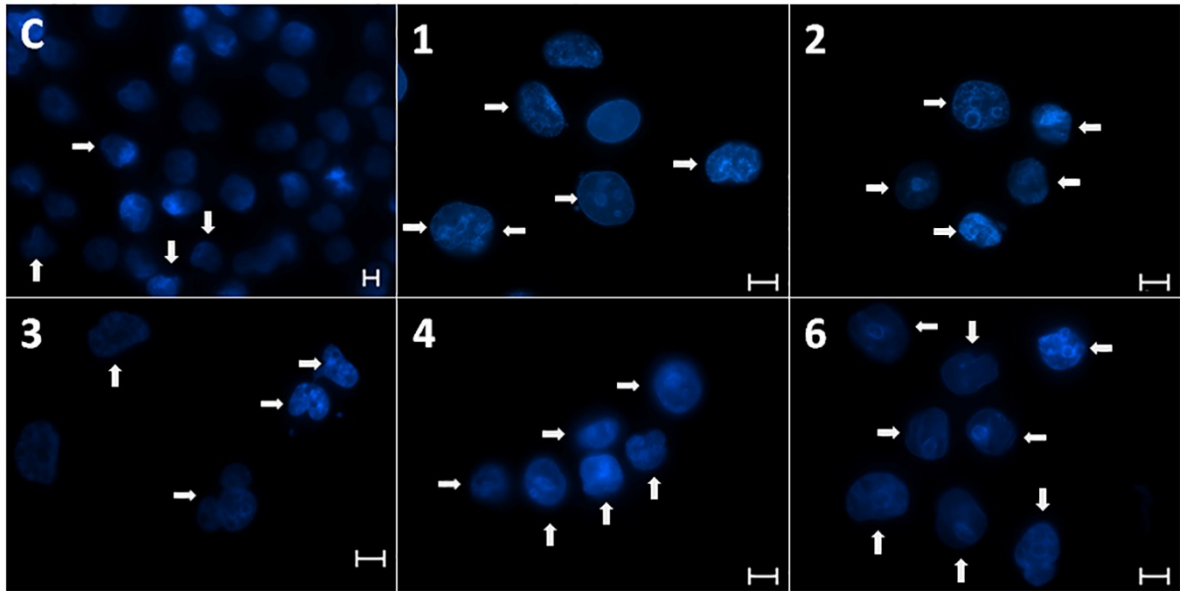

Figure S22. Induction of apoptosis by complexes **1**-**4**, **6**. Representative images of HCT116 cells incubated for 48 h with the IC_{50} concentrations of complexes **1**-**4** and **6** and the control vehicle (0.1% (v/v) DMSO; C), depicting cells with morphological changes characteristic of cells in apoptosis (white arrows). The white scale bar indicates 10 μm.

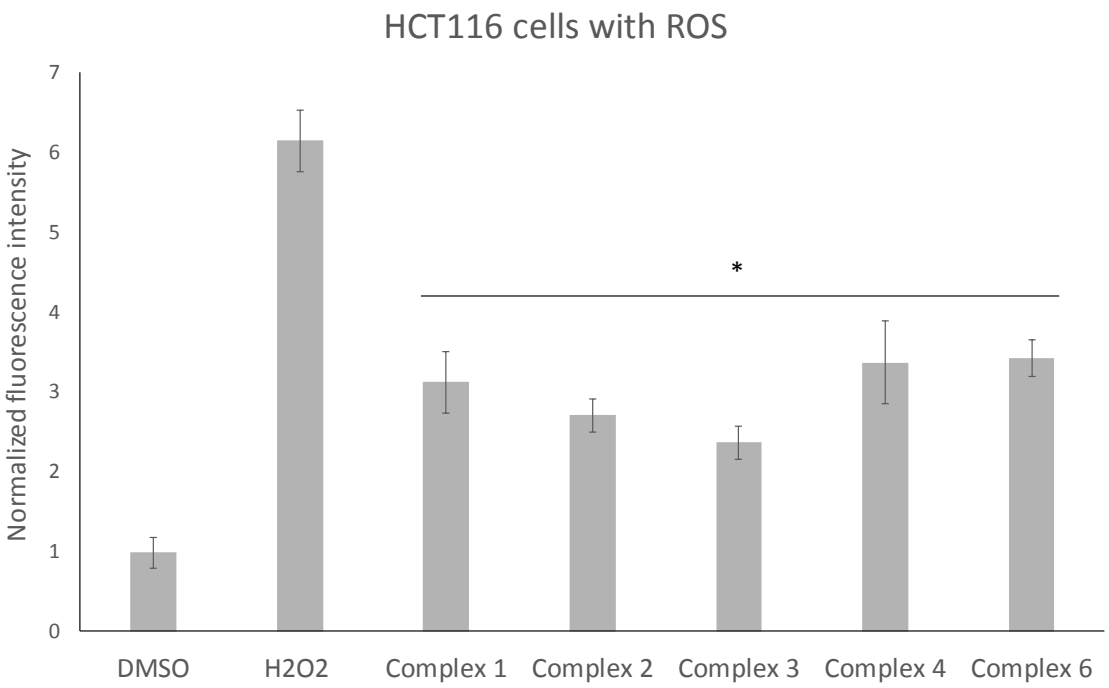

Figure S23. Induction of Reactive Oxygen Species (ROS) in HCT116 cells incubated with IC_{50} concentrations of metallic complexes **1-4** and **6** for 48 h measured by the 2',7'-dichlorodihydrofluorescein diacetate (H_2DCF-DA) method. The results shown are expressed the mean fluorescence intensity of each sample normalized to the fluorescence intensity of control cells exposed to 0.1% (v/v) DMSO (vehicle control). Results are expressed as the average ± SD from three independent assays. Hydrogen peroxide (H_2O_2) was used as positive control. The symbol * means that the results are statistically significant with a $p < 0.0001$ (as compared to the 0.1% (v/v) DMSO control).